Volume. 2., 2012 ISSN 2253-0371

Annual Review of Chaos Theory, Bifurcations and Dynamical Systems

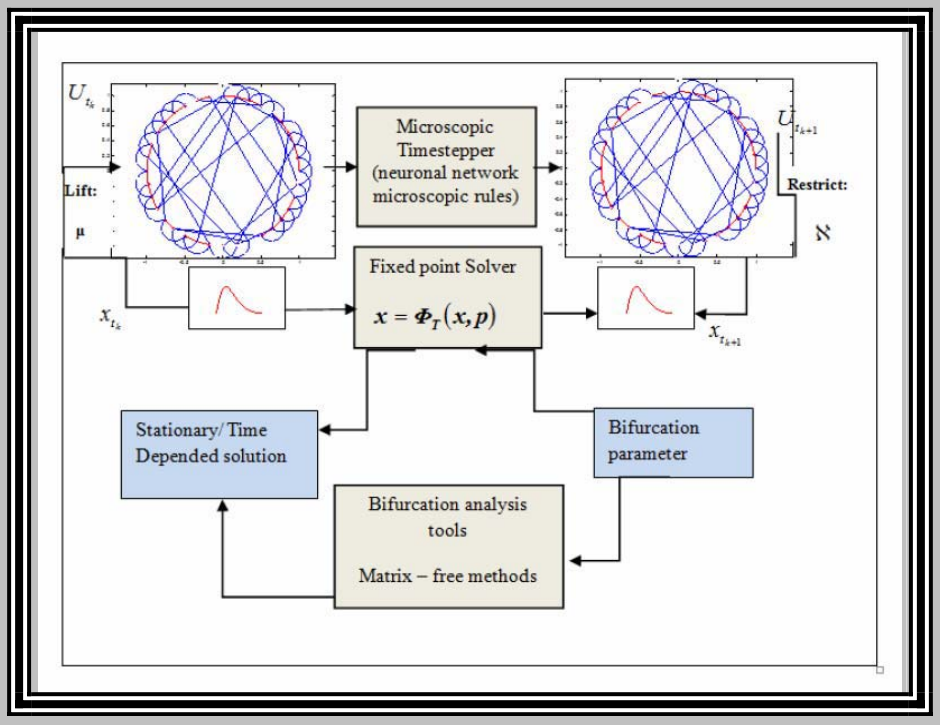

Annual Review of Chaos Theory, Bifurcations and Dynamical Systems

Aims and scope

Annual Review of Chaos Theory, Bifurcations and Dynamical Systems (*ARCTBDS*) (www.arctbds.com) is a multidisciplinary international peer reviewed journal of chaos theory, bifurcations and dynamical systems publishing high-quality articles quarterly. The primary objective of this review journal is to provide a forum for this multidisciplinary discipline of chaos theory, bifurcations and dynamical systems as well as general nonlinear dynamics. This review journal will be a periodical or series that is devoted to the publication of review (and original research) articles that summarize the progress in particular areas of chaos theory, bifurcations and dynamical systems during a preceding period. Also, the journal publishes original articles and contributions on the above topics by leading researchers and developers.

Subject Coverage

Annual Review of Chaos Theory, Bifurcations and Dynamical Systems (*ARCTBDS*) (www.arctbds.com) covers all aspects of chaos theory, bifurcations and dynamical systems. Topics of interest include, but are not limited to:

- Mathematical modeling, computational methods, principles and numerical simulations
- Chaos, bifurcation, nonlinear dynamical systems, complexity in nonlinear science and engineering and numerical methods for nonlinear differential equations.
- Fractals, pattern formation, solitons, coherent phenomena and nonlinear fluid dynamics.
- Control theory and stability and singularity on fundamental or applied studies.
- Real applications in all areas of science.

Papers can be oriented towards theory, algorithms, numerical simulations, applications or experimentation.

Readership and audience

Advanced undergraduates and graduate students in natural and human sciences and engineering such as physics, chemistry, biology or bioinformatics…etc; academics and practitioners in nonlinear physics and in various other areas of potential application; researchers, instructors, mathematicians, nonlinear scientists and electronic engineers interested in chaos, nonlinear dynamics and dynamical systems and all interested in nonlinear sciences.

Annual Review of Chaos Theory, Bifurcations and Dynamical Systems

Submission of Papers

Manuscripts should be in English and should be written in a LaTeX file only. All submissions should be sent electronically to the journal website:

http://www.easychair.org/conferences/?conf=arctbds

The other formats are not acceptable. Authors are advised to keep a copy of their manuscript since the journal cannot accept responsibility for lost copies. The submitted papers to this journal should not have been previously published nor be currently under consideration for publication elsewhere. All papers are refereed through a double blind process. There is no financial reward for reviewers and editors of this journal. These positions are purely voluntary. When the manuscript is accepted for publication, the authors agree to automatic transfer of the copyright to the journal. The manuscript should contain the following items: An informative title, author's name, address and e-mail, abstract, 3-5 keywords, text, conclusion, and references. Footnotes should be avoided if possible. References should be denoted in the text by numbers in square brackets, e.g. [10]. References should be complete, in the following style:

- **Papers:** Author(s) initials followed by last name for each author, "paper title," publication name, volume, inclusive page numbers, month and year. Authors should consult Mathematical Reviews for standard abbreviations of journal names..
- **Books:** Author(s), title, publisher, location, year, chapter or page numbers (if desired).
- **Each figure and table or any material** (i.e., Fig. 10, Table. 1, ...etc) should be mentioned in the text and numbered consecutively using Arabic numerals. Number each table consecutively using Arabic numerals. Type a brief title below each figure and table or any material. Figures should be submitted separately as encapsulated postscript (.eps) files.

For accepted papers, the author(s) will be asked to transfer copyright of the article to the journal. The manuscript will not be published until the **Copyright Transfer Form** is received.

Page proofs will be sent to the corresponding author. The proofs must be corrected and returned within three days of receipt. **There are no charges for publishing in this journal and each author will receive a PDF copy of his/her paper.**

Contribution Enquiries and Submitting

Editorial office (Algeria office): Annual Review of Chaos Theory, Bifurcations and Dynamical Systems (ARCTBDS) Dr. Zeraoulia Elhadj, Department of Mathematics, University of Tébessa, (12002), Algeria, e-mail: zeraoulia@mail.univ-tebessa.dz and zelhadj12@yahoo.fr.

Annual Review of Chaos Theory, Bifurcations and Dynamical Systems

Annual Review of Chaos Theory, Bifurcations and Dynamical Systems

Annual Review of Chaos Theory, Bifurcations and Dynamical Systems

Volume. 2., 2012

Table of Contents

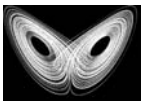

Annual Review of Chaos Theory, Bifurcations and Dynamical Systems
Vol. 2, (2012) 1-20, www.arctbds.com.

Symmetry and Symmetry-Breaking of the Emergent Dynamics of the Discrete Stochastic Majority-Voter Model

K. G. Spiliotis
School of Applied Mathematics and Physical Sciences
National Technical University of Athens, Greece
e-mail: spiliotiskos@gmail.com

L. Russo
Istituto di Ricerche sulla Combustione
Consiglio Nazionale delle Ricerche, Naples, Italy
e-mail: lrusso@irc.cnr.it

C. I. Siettos
School of Applied Mathematics and Physical Sciences
National Technical University of Athens, Greece
e-mail: ksiet@mail.ntua.gr

Abstract

We analyse the emergent dynamics of the so called majority voter model evolving on complex networks. In particular we study the influence of three characteristic types of networks, namely Random Regular, Erdös-Rényi (ER), Watts and Strogatz (WS, small-world) and Barabasi (scale- free) on the bifurcating stationary coarse-grained solutions. We first prove analytically some simple properties about the symmetry and symmetry breaking of the macroscopic dynamics with respect to the network topology. We also show how one can exploit the Equation-free framework to bridge in a computational strict manner the micro to macro scales of the dynamics of stochastic individualistic models on complex random graphs. In particular, we show how systems-level tasks such as bifurcation analysis of the coarse-grained dynamics can be performed bypassing the need to extract macroscopic models in a closed form. A comparison with the mean-field approximations is also given illustrating the merits of the Equation-Free approach, especially in the case of scale-free networks exhibiting a heavy-tailed connectivity distribution.

Keywords: Majority-Voter Model, Micro to Macro bridging, Coarse-grained computations, Equation-free approach, Complex Networks, Nonlinear Dynamics.

Manuscript accepted April 20, 2012.

1 Introduction

Social-like mimetic behavior - otherwise described as trend following or majority-voter or majority-rule- has been, over the last century, a key factor in determining and shaping economical and political changes around the world [20, 45, 23]. Taking as an example decision making, it has been demonstrated that the mimetic behavior of individuals may significantly affect rational decisions under incomplete information [39, 37, 49, 16]. Identifying and understanding collective actions from such phenomena has therefore been an important research task for psychologists, sociologists and economists. Over the years, scientists have extensively used this mechanism to model and gain a better understanding on the behavior of opinion formation and voter/election dynamics [8, 19, 48, 7, 32, 33] culture and language dynamics [11, 3, 6, 10, 35], crowd flow design and management [18, 21, 17, 40], diffusion of news and innovations [15, 34, 51],but also epidemic spread dynamics [5, 4, 13, 28, 27, 42] ecology [24] and neuroscience [31, 46, 47]. Given the nature of the process, it is clear that the network topology, on which the interaction of the individuals evolves, can shape the emergent macroscopic dynamics. However, it is less clear how one can quantify in a systematic manner the dependence of the emergent dynamics with respect to both network characteristics and model parameters. Due to the nonlinear, stochastic nature of such models and their coupling to complex network structures, the emergent behavior cannot be-most of the times-accurately modeled and analyzed in a straightforward manner.

While one can try to use the tools of statistical physics to write down coarse-grained master equations to describe the probabilistic time evolution of the macroscopic quantities for simple-structured homogeneous networks (in the sense that there is a constant degree connectivity and/or that the structure is poorly clustered), major problems arise in trying to find fair- or perform computations based on- macroscopic models in a closed form when dealing with complex heterogeneous networks (such as scale-free type of networks) [50, 1, 38]. This imposes a major obstacle to systems-level computational tasks, such as bifurcation and stability analysis which rely on the availability of efficient low-order closed models written in terms of a few macroscopic (coarse-grained) variables. Hence, being able to systematically analyze the dynamics of majority-voter processes on complex networks becomes, in this context, of great importance.

Here, our main focus is to systematically explore the dynamics of the basic majority-voter process deploying on complex networks. We first prove analytically some symmetry properties of the corresponding mean field models. We then show how the network structure induces symmetry breaking of the system solutions giving rise to hysteresis phenomena. Asymmetric behavior predicted by detailed network models has been observed in many real-world complex problems. In particular, symmetry breaking of majority-voter

processes has been related to phenomena such as herd behavior under panic [2], the emergence of cooperation dynamics [41] and public opinion formation [22]. Finally, in order to systematically analyse the way symmetry breaking influences the emergent dynamics we exploit the Equation-Free framework [29, 14, 44, 36] bypassing the construction of explicit coarse-grained models. In particular, we construct the coarse-grained bifurcation diagrams and perform a stability analysis of the basic majority-rule dynamics evolving on complex networks, with respect to (a) model's switching-state probability and (b) to the underlying degree distribution. We should note that this is the first time that such an analysis is provided using the detailed stochastic model in an explicit manner, i.e. bypassing the need to construct mean-field approximations. A comparison with the mean field approximations is also demonstrated, to reveal the merits of the proposed framework. In particular in the case of scale-free structures even if one manages to extract exact mean filed approximations, we show that bifurcation analysis, based on the corresponding analytical mean field approximation, appears to be an overwhelming difficult task, due to the heavy tail power-law connectivity distribution.

The paper is organized as follows. In section 2 we describe the majority-voter model deploying on a network while in section 3 we prove analytically how the connectivity degree of random graphs governs the symmetry and the symmetry breaking of the solutions of the corresponding mean field models. In section 4 we derive the mean field approximation of the majority-voter model in the case of complex networks with arbitrary degree distributions. In section 5, we show how the Equation-free framework can be exploited to perform systems level tasks on complex networks. In section 6 we present the results of the coarse-grained numerical analysis, constructing the coarse-grained bifurcation diagrams of the majority-voter dynamics as these obtained by exploiting the Equation-free approach on complex networks. A comparison with the bifurcation diagrams obtained using the mean field approximations is also made. We conclude in section 7.

2 The discrete stochastic majority-voter model

In our simple basic majority-voter model [31, 46, 47], each individual is labeled as i, (i=1,2,...,N), which votes for "A" or "B". Hence, the state of the i-*th* individual in time is described with the function $a_i(t) \in \{0, 1\}$, where the values 1 and 0 corresponds to "A" and "B" selection respectively. Let us denote by $\Lambda(i)$ the set of the neighbors (i.e. the individuals connected to i-*th* individual, with self loop included). The summation

$$\sigma_i(t) = \sum_{j \in \Lambda(i)} a_i(t) \tag{1}$$

gives the number of individuals socially linked with the i-*th* individual voting for "A". At each time step each individual is influenced by its social interactions, and changes its preference according to the following simple stochastic rules:

1. A "B" voter changes its preferences to "A" with probability ε, if $\sigma_i(t) \leq \left(\frac{k_i}{2}\right)$ (where k_i is the degree of the $i-th$ individual). If $\sigma_i(t) > \left(\frac{k_i}{2}\right)$ the individual keeps changes its preferences to "A" with probability $1 - \varepsilon$.

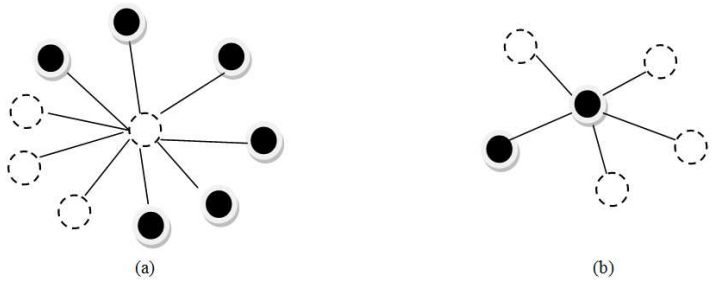

Figure 1: An example of the majority-voter rules. The open circle represents a "B" voter, while the filled circle represents an "A" voter (a). $p_{B\to A} = 1-\varepsilon$, since $\sigma(t) = \sum_{j=1}^{10} a_j(t) = 6 > degree(i)/2$. Here $degree$(i)=10 (self loop is included). (b) Similar, $p_{A\to B} = 1-\varepsilon$, since $\sigma(t) = \sum_{j=1}^{6} a_j(t) = 2 < degree(i)/2$.

2. An individual with a preference "A" changes its preference to "B" with probability ϵ, if $\sigma_i(t) > \left(\frac{k_i}{2}\right)$. If $\sigma_i(t) \leq \left(\frac{k_i}{2}\right)$, the individual changes its preference to B with probability $1-\varepsilon$. The probability ε ranges in $(0, 0.5)$. We illustrate the operation of the above rules in Fig. 1.

3 Symmetry and symmetry breaking of the solutions of the mean-field majority-voter model evolving on random regular networks (RRN)

In the following section we prove some simple but important properties of the majority-voter dynamics evolving on random regular networks.

3.1 RRN with an odd connectivity distribution

For our analysis we start by considering a random network with constant, odd, connectivity degree: $k = 2l-1$ and $l \in N$ (self loop is included). In this case, the time evolution of the density of A voters is given by the equation

$$d_{t+1} = f_{2l-1}(d_t) \tag{2}$$

where the function f_{2l-1} takes the form

$$f_{2l-1}(d,\varepsilon) = (1-\varepsilon)(\binom{2l-1}{0}d^{2l-1} + \binom{2l-1}{1}d^{2l}(1-d) + ... + \binom{2l-1}{l-1}d^{l}(1-d)^{l-1}) + \\ + \varepsilon(\binom{2l-1}{l}d^{l-1}(1-d)^{l} + \binom{2l-1}{l+1}d^{l-2}(1-d)^{l+1} + ... + \binom{2l-1}{2l-1}(1-d)^{2l-1}) \tag{3}$$

In this case, the following proposition holds:

Proposition 3.1.1. *Let (G, E) be a network with constant odd connectivity $k = 2l - 1$, $l \in N$. Then the fixed point solutions of equation (2) for a constant ε are symmetric with respect to $d = 1/2$.*

Proof. We shall prove that if d_0 is a solution of Eq. (2), then $1 - d_0$ is also a solution. The function f_{2l-1}, Eq. (3) can be written in a more compact form

$$f_{2l-1}(d,\varepsilon) = (1-\varepsilon)\sum_{i=0}^{l-1}\binom{2l-1}{i}d^{2l-1-i}(1-d)^i + \varepsilon\sum_{i=l}^{2l-1}d^{2l-1-i}(1-d)^i \tag{4}$$

Eq. (4) can be put in the following form

$$f_{2l-1}(d,\varepsilon) = (1-\varepsilon)f_{1,2l-1}(d) + \varepsilon f_{2,2l-1}(d) \tag{5}$$

where

$$f_{1,2l-1}(d) = \sum_{i=0}^{l-1}\binom{2l-1}{i}d^{2l-1-i}(1-d)^i \tag{6}$$

and

$$f_{2,2l-1} = \sum_{i=l}^{2l-1}\binom{2l-1}{i}d^{2l-1-i}(1-d)^i. \tag{7}$$

The fixed point solutions of Eq. (2) are derived from

$$d = f_{2l-1}(d,\varepsilon) \Leftrightarrow d - f_{2l-1}(d,\varepsilon) = 0 \Leftrightarrow G_{2l-1}(d,\varepsilon) = 0 \tag{8}$$

and

$$G_{2l-1}(d,\varepsilon) = d - f_{2l-1}(d,\varepsilon) \tag{9}$$

Any solution d_0 of Eq. (8)satisfies

$$d_0 = f_{2l-1}(d_0,\varepsilon) \Leftrightarrow d_0 = (1-\varepsilon)f_{1,2l-1}(d_0) + \varepsilon f_{1,2l-1}(d_0) \tag{10}$$

□

Remark 3.1.2. *$f_{1,2l-1}(1-d) = f_{2,2l-1}(d)$ and $f_{2,2l-1}(1-d) = f_{1,2l-1}(d)$*

Proof.

$$\begin{aligned} f_{1,2l-1}(1-d) = \sum_{i=0}^{l-1}\binom{2l-1}{i}(1-d)^{2l-1-i}d^i = \binom{2l-1}{0}(1-d)^{2l-1} \\ + \binom{2l-1}{1}(1-d)^{2l-1-1}d + ... + \binom{2l-1}{l-1}(1-d)^l d^{l-1} \end{aligned}$$

It is known that $\binom{n}{k} = \binom{n}{n-k}$ for $0 \le k \le n$ hence

$$\begin{aligned} f_{1,2l-1}(1-d) = \binom{2l-1}{2l-1}(1-d)^{2l-1} + \binom{2l-1}{2l-2}(1-d)^{2l-2}d + \\ ... + \binom{2l-1}{l}(1-d)^l d^{l-1} = \sum_{i=l}^{2l-1}\binom{2l-1}{i}d^{2l-1-i}(1-d)^i \\ = f_{2,2l-1}(d) \end{aligned}$$

Remark 3.1.3. $f_{1,2l-1}(d) + f_{2,2l-1}(d) = 1$

Proof.

$$f_{1,2l-1}(d) + f_{2,2l-1}(d) = \sum_{i=0}^{l-1} \binom{2l-1}{i} d^{2l-1-i}(1-d)^i + \sum_{i=l}^{2l-1} \binom{2l-1}{i} d^{2l-1-i}(1-d)^i$$
$$= \sum_{i=0}^{2l-1} \binom{2l-1}{i} d^{2l-1-i}(1-d)^i = (d+1-d)^{2l-1} = 1^{2l-1} = 1 \quad (11)$$

□

Putting in the expression of G, Eq. (8), $d_0 \to 1 - d_0$ we get

$$G_{2l-1}(1-d_0, \varepsilon) = 1-d_0-f_{2l-1}(1-d_0, \varepsilon) = 1-d_0-(1-\varepsilon)f_{1,2l-1}(1-d_0)-\varepsilon f_{2,2l-1}(1-d_0) \quad (12)$$

Substituting the expression of d_0 from Eq. (10) in Eq. (12) we get

$$G_{2l-1}(1-d_0, \varepsilon) = 1-(1-\varepsilon)f_{1,2l-1}(d_0) - \varepsilon f_{2,2l-1}(d_0) - (1-\varepsilon)f_{1,2l-1}(1-d_0) - \varepsilon f_{2,2l-1}(1-d_0) \quad (13)$$

and by remark 3.1.2

$$G_{2l-1}(d_0, \varepsilon) = 1-(1-\varepsilon)f_{1,2l-1}(d_0) - \varepsilon f_{2,2l-1}(d_0) -$$
$$(1-\varepsilon)f_{2,2l-1}(d_0) - \varepsilon f_{1,2l-1}(d_0) = 1-(f_{1,2l-1}(d_0) + f_{2,2l-1}(d_0)) = 1-1 = 0$$

□

Proposition 3.1.4. *For each ε, and for constant odd connectivity there is always the solution $d_0 = \frac{1}{2}$.*

Proof.

$$G_{2l-1}(\frac{1}{2}, \varepsilon) = \frac{1}{2} - f_{2l-1}(\frac{1}{2}, \varepsilon) = \frac{1}{2} - (1-\varepsilon)f_{1,2l-1}(\frac{1}{2}) - \varepsilon f_{2,2l-1}(\frac{1}{2}) \quad (14)$$

from remark 3.1.2, putting $d = \frac{1}{2}$ we get that

$$f_{1,2l-1}(\frac{1}{2}) = f_{2,2l-1}(\frac{1}{2}) \quad (15)$$

therefore

$$G_{2l-1}(\frac{1}{2}, \varepsilon) = \frac{1}{2} - (1-\varepsilon+\varepsilon)f_{1,2l-1}(\frac{1}{2})$$
$$= \frac{1}{2} - f_{1,2l-1}(\frac{1}{2}) = \frac{1}{2} - \sum_{i=0}^{l-1} \binom{2l-1}{i} \frac{1}{2}^{2l-1-i} (\frac{1}{2})^i =$$
$$= \frac{1}{2} - \sum_{i=0}^{l-1} \binom{2l-1}{i} (\frac{1}{2})^{2l-1} = \frac{1}{2} - (\frac{1}{2})^{2l-1} \sum_{i=0}^{l-1} \binom{2l-1}{i} =$$
$$= \frac{1}{2} - (\frac{1}{2})^{2l-1} 2^{2l-2} = \frac{1}{2} - \frac{1}{2} = 0 \quad (16)$$

□

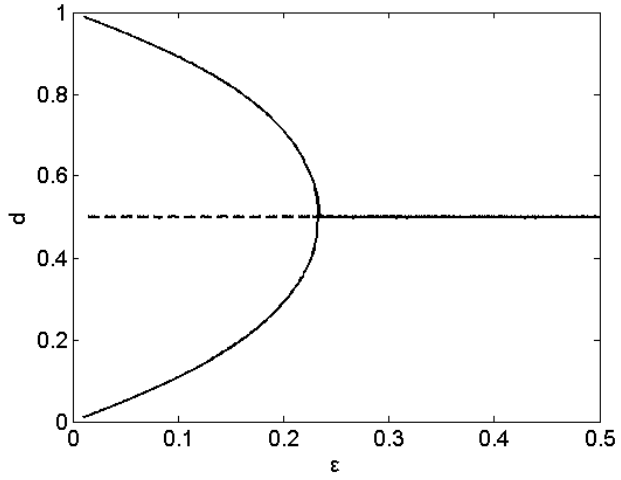

Figure 2: Bifurcation diagram of the density of "A" voters with respect to the switching probability ε, as constructed using the mean field approximation of the majority-voter dynamics evolving one a RRN with a constant degree distribution equal to 5 (as produced using Eq. (8)).

Fig. 2 gives the bifurcation diagram for a random network with constant connectivity degree equal to 5 (self loop is included), resulting from Eq. 8. Clearly there are two branches of symmetric solutions around the steady solution $d_0 = \frac{1}{2}$.

Now suppose that the network has a degree distribution $P(k)$ containing only odd degrees. Specifically, let us assume that the network has N_1 nodes with a degree equal to $2l_1 - 1$, N_2 nodes with a degree equal to $2l_2 - 1$,..., N_k nodes with degree equal to $2l_k - 1, (N_1 + N_2 + ... + N_k = N$ and $l_i \in \ N, i = 1, 2, ...k)$. The time evolution of the density can be split into sums of conditional probabilities of specific degrees:

$$d_{t+1} = f_{tot}(d_t, \varepsilon) \tag{17}$$

and

$$f_{tot}(d_t, \varepsilon) = \sum_{i=1}^{k} f_{2l_i-1}(d, \varepsilon) P(2l_i - 1) \tag{18}$$

The fixed point solution of Eq. (17) is

$$d = f_{tot}(d, \varepsilon) \Leftrightarrow d - f_{tot}(d, \varepsilon) = 0 \Leftrightarrow G_{tot}(d, \varepsilon) = 0 \tag{19}$$

Now we will prove the following

Proposition 3.1.5. *Let (G, E) be a network with a degree distribution containing only odd dergees Then the fixed point equation, Eq. (19), for a constant ε, has symmetric solutions with respect to $d = 1/2$.*

Proof. Suppose that d_0 is a solution of Eq. 19. Then

$$d_0 = \sum_{i=1}^{k} f_{2l_i-1}(d_0, \varepsilon) P(2l_i - 1) \tag{20}$$

From the proof of proposition 3.1.1 we have that for each $i, (i = 1, 2, ..., k)$ the function f_{2l_i-1} can be written as a convex combination of two other functions $f_{1,2l_i-1}$ and $f_{2,2l_i-1}$ (Eq. 5) i.e.

$$f_{2l_i-1}(d, \varepsilon) = (1-\varepsilon) f_{1,2l_i-1}(d) + \varepsilon f_{2,2l_i-1}(d) \tag{21}$$

By remark 3.1.2 we have

$$f_{1,2l_i-1}(1-d) = f_{2,2l_i-1}(d) \tag{22}$$

and

$$f_{2,2l_i-1}(1-d) = f_{1,2l_i-1}(d) \tag{23}$$

Now we set $d_0 \to 1 - d_0$ in the function G_{tot} Eq. (19) to get

$$G_{tot}(1-d_0, \varepsilon) = 1 - d_0 - f_{tot}(1-d_0, \varepsilon) = 1 - d_0 - \sum_{i=1}^{k} f_{2l_i-1}(1-d_0, \varepsilon) P(2l_i - 1) =$$

$$= 1 - d_0 - \sum_{i=1}^{k} ((1-\varepsilon) f_{1,2l_i-1}(1-d_0) + \varepsilon f_{2,2l_i-1}(1-d_0)) P(2l_i - 1) \tag{24}$$

Substituting Eq. (20) in Eq. (24) we get that:

$$\begin{cases} G_{tot}(1-d_0, \varepsilon) = 1 - \sum_{i=1}^{k} f_{2l_i-1}(d_0, \varepsilon) P(2l_i - 1) \\ - \sum_{i=1}^{k} ((1-\varepsilon) f_{1,2l_i-1}(1-d_0) + \varepsilon f_{2,2l_i-1}(1-d_0)) P(2l_i - 1) \\ = 1 - \sum_{i=1}^{k} ((1-\varepsilon) f_{1,2l_i-1}(d_0) + \varepsilon f_{2,2l_i-1}(d_0)) P(2l_i - 1) \\ - \sum_{i=1}^{k} ((1-\varepsilon) f_{1,2l_i-1}(1-d_0) + \varepsilon f_{2,2l_i-1}(1-d_0)) P(2l_i - 1) \\ = 1 - \sum_{i=1}^{k} ((1-\varepsilon) f_{1,2l_i-1}(d_0) + \varepsilon f_{2,2l_i-1}(d_0) \\ + (1-\varepsilon) f_{2,2l_i-1}(d_0) + \varepsilon f_{1,2l_i-1}(d_0)) P(2l_i - 1) \\ = 1 - \sum_{i=1}^{k} (f_{1,2l_i-1}(1-d_0) + f_{2,2l_i-1}(1-d_0)) P(2l_i - 1) \end{cases} \tag{25}$$

Taking into account that $f_{1,2l_i-1}(d) + f_{2,2l_i-1}(d_0) = 1$ and $\sum_{i=1}^{k} P(2l_i - 1) = 1$, the last expression of Eq. (25) reads:

$$G_{tot}(1-d_0, \varepsilon) = 1 - \sum_{i=1}^{k} (f_{1,2l_i-1}(1-d_0) + f_{2,2l_i-1}(1-d_0)) P(2l_i - 1) =$$

$$= 1 - \sum_{i=1}^{k} P(2l_i - 1) = 1 - 1 = 0 \tag{26}$$

□

Fig. 3 gives the bifurcation diagram for a random network with the degree distribution contains only odd degrees, resulting from Eq. (19). The two branches of symmetric solutions around the steady solution $d_0 = \frac{1}{2}$ still exist.

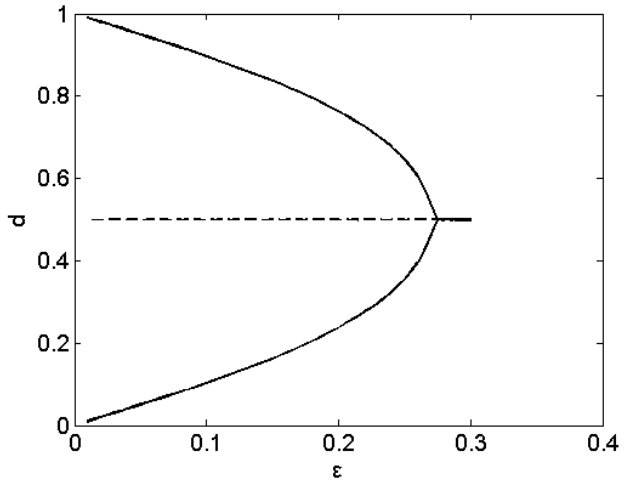

Figure 3: Bifurcation diagram of the density of "A" voters with respect to the switching probability ε, as constructed using the mean-field approximation of the majority-voter dynamics evolving on networks containing only odd degrees (here 5, 7, 9) (as produced using Eq. (18), (19)).

3.2 RRN with even connectivity distribution

In the general case of a network (G, E) with arbitrary even constant connectivity degree, the time evolution of the density reads:

$$d_{t+1} = f_{2l}(d_t, \varepsilon) \tag{27}$$

with

$$f_{2l}(d,\varepsilon) = (1-\varepsilon)\sum_{i=0}^{l-1}\binom{2l}{i}d^{2l-i}(1-d)^i + \varepsilon\sum_{i=l}^{2l}\binom{2l}{i}d^{2l-i}(1-d)^i \tag{28}$$

Eq. (28) can be written as

$$f_{2l}(d,\varepsilon) = (1-\varepsilon)f_{1,2l}(d) + f_{2,2l}(d) + \varepsilon\binom{2l}{l}d^l(1-d)^l \tag{29}$$

where $f_{1,2l}(d) = \sum_{i=0}^{l-1}\binom{2l}{i}d^{2l-i}(1-d)^i$ and $f_{2,2l}(d) = \sum_{i=0}^{l-1}\binom{2l}{i}d^{2l-i}(1-d)^i$. Similar to the proof of remark 3.1.2, the two parts $f_{1,2l}(d)f_{2,2l}(d)$, are symmetric with respect to $d = \frac{1}{2}$. Due to the perturbation term $\varepsilon\binom{2l}{l}d^l(1-d)^l$ the function loses its symmetry, resulting to the symmetry breaking of the corresponding bifurcation diagram of Eq. (27), (Fig. 4).

4 The mean field majority-voter model dynamics in networks with arbitrary degree distribution

In order to extract the mean field approximation for complex networks with arbitrary degree distributions, we choose at random a node i. Let k be the degree of the i-*th* node

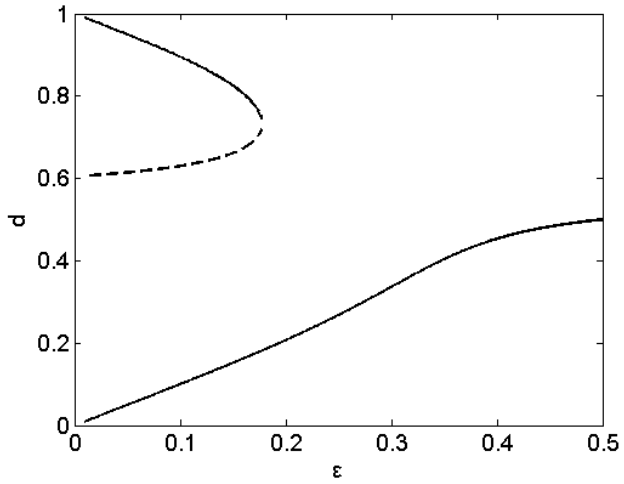

Figure 4: Bifurcation diagram of the density of A voters with respect to the switching probability, as constructed using the mean field approximation of the majority-voter dynamics evolving on a RRN with constant degree distribution equal to 8 (as produced using Eq. (28) and the fixed point solution of Eq. (27)).

and d_t be the density of A voters on the network at time t. Then, the probability of the i-th individual (with degree k) to have a preference A at the next time step $t+1$ is

$$f_k(d_t,\varepsilon)=\sum_{n=0}^{k}a(k,\varepsilon)\binom{k}{n}d_t^{k-n}(1-d_t)^n \tag{30}$$

where $a(k,\varepsilon)=\begin{cases}\varepsilon, if n\leq\frac{k_{max}}{2}\\ 1-\varepsilon, else\end{cases}$. Let $f(d_t,\varepsilon)$ be the probability at time $t+1$ a randomly chosen zero node, to become one. Then

$$f(d_t,\varepsilon)=\sum_{k=1}^{kmax}f_k(d_t,\varepsilon)P(k) \tag{31}$$

where $P(k)$ be the connectivity degree distribution. The time evolution of the switching probability reads

$$d_{t+1}=f(d_t,\varepsilon) \tag{32}$$

For the computation of the stationary points one has to solve the following fixed-point equation:

$$d-f(d,\varepsilon)=0\Leftrightarrow G(d,\varepsilon)=0 \tag{33}$$

For complex networks with a high heterogeneity in the connectivity distribution (such as scale free networks) the fixed point solution of Eq. (33), given Eq. (30) and Eq(31) may become a non-trivial computational task as for a degree distribution with heavy nodes one needs to compute polynomial coefficients of the order of $\binom{k}{n}$.

5 The Equation-free approach for multi-scale computations on complex heterogeneous networks

For detailed individualistic/ stochastic models whose dynamics deploy on heterogeneous networks, the derivation of explicit efficient macroscopic representations for the emergent dynamics in a closed form is most of the times an overwhelming difficult task. The Equation-free approach can be used to bypass the need for extracting explicit continuum models in closed form [29, 14, 44, 36, 30, 43, 25]. The key assumption of the methodology is that a macroscopic model for the emergent dynamics exists and closes in terms of a few coarse-grained variables. These coarse-grained variables are usually the low-order moments of the detailed evolving distribution over the networks. What the methodology does, in fact, is to provide closures on demand in a computational manner. The methodology can be described by the following steps (see also Fig. 5):
(a) Choose the coarse-grained statistics, say $\boldsymbol{x}$, for describing the emergent behavior of the system and an appropriate representation for them (for example the mean value of the underlying evolving distribution).
(b) Choose an appropriate lifting operator μ that maps to a detailed distribution $\mathbf{U}$ on the network. (For example, μ could make random state assignments over the network which are consistent with the densities).
(c) Prescribe a continuum initial condition at a time t_k, say, $\mathbf{x}_{t_k}$.
(d) Transform this initial condition through lifting to N consistent individual-based realizations $\mathbf{U}_{t_k} = \mu\mathbf{x}_{t_k}$.
(e) Evolve these N realizations for a desired time T, generating the $\mathbf{U}_{t_{k+1}}$, where $t_k = kT$.
(f) Obtain the restrictions $x_{t_{k+1}} = \aleph\mathbf{U}_{t_k}$.
The above steps, constitute the so called *coarse timestepper*, which, given an initial coarse-grained state of the system $\mathbf{x}_{t_k}$ at time t_k reports the result of the integration of the model over the network after a given time-horizon T (at time t_{k+1}), i.e.

$$\mathbf{x}_{t_{k+1}} = \Phi_T(\mathbf{x}_{t_k}, \mathbf{p}). \tag{34}$$

where $\Phi_T : R^n \times R^m \to R^n$ having $\mathbf{x}_k$ as initial condition.

The existence of a coarse-grained the temporal evolution operator, Φ_{T_h}, which is assumed to be unavailable analytically in a closed form, implies that the higher order moments of the distributions become, relatively quickly, slaved to the lower, few, slow ones.

At this point one can implement around the coarse-grained input-output map Eq. (34), a fixed point iterative scheme order to compute fixed point or periodic solutions at certain values of the parameter space. For example for low-order systems coarse-grained equilibria can be obtained as fixed points, of the map :

$$\mathbf{x} - \Phi_T(\mathbf{x}, \mathbf{p}) = 0. \tag{35}$$

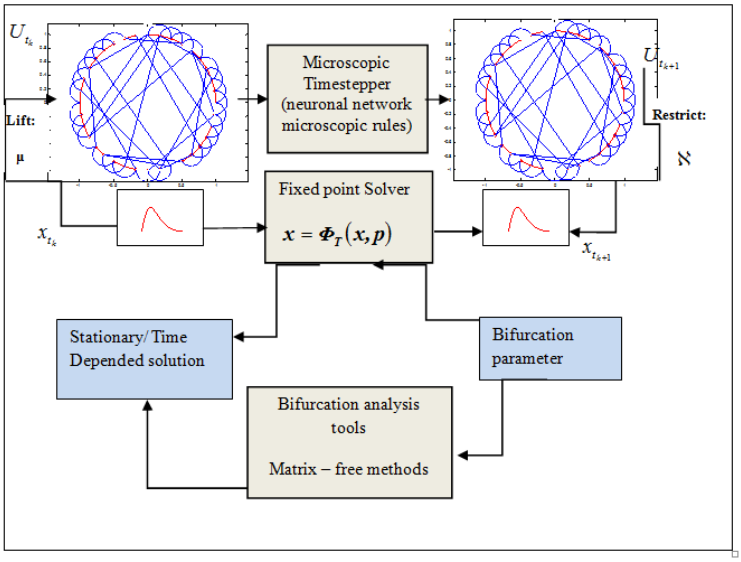

Figure 5: Schematic description of the concept of the Equation-Free approach.

6 Coarse-Grained Numerical analysis using the Equation-free approach

The results are obtained using networks of $N = 10000$ individuals. We performed a coarse-grained analysis for ER, WS and scale-free networks [1, 12, 50, 38]. The coarse-grained bifurcation diagrams, with respect to the switching probability parameter ε, were constructed exploiting the Equation-free framework as described in the previous section. Our coarse-grained variable is the density d of the A voters. At time t_0, we created N_{copies} different distribution realizations consistent with the macroscopic variable d . The coarse timestepper is constructed as the T-map:

$$d_{t+1} = \Phi_T(d_t, \varepsilon) \tag{36}$$

The derived coarse-grained bifurcation diagrams are depicted in Fig. 6-8 respectively. The stationary states on the coarse-grained bifurcation diagram have been obtained as fixed points of Eq. (35) averaging over $N_{copies} = 10000$ realizations. Continuation around the coarse-grained turning points is accomplished by solving the Eq. (35) augmented by the pseudo-arc-length continuation, i.e.:

$$\begin{cases} G(d,\varepsilon) = d - \Phi(d,\varepsilon) = 0 \\ N(D,\varepsilon) = a(d-d_1) + b(\varepsilon - \varepsilon_1) - ds = 0 \end{cases} \tag{37}$$

where $a = \frac{d_1 - d_0}{ds}$ and $b = \frac{\varepsilon_1 - \varepsilon_0}{ds}$ and is the pseudo arc-length continuation step. The ordered pairs (d_0, ε_0) and (d_1, ε_1) are two already computed solutions. The computation of the fixed points can now be obtained using an iterative procedure like the Newton-Raphson technique.The procedure involves the iterative solution of the following linearized system:

$$\begin{bmatrix} 1 - \frac{\partial \Phi_T}{\partial d} & -\frac{\partial \Phi_T}{\partial \varepsilon} \\ a & b \end{bmatrix} \begin{bmatrix} \delta d \\ \delta \varepsilon \end{bmatrix} = \begin{bmatrix} d - \Phi_T(d,\varepsilon) \\ N(d,\varepsilon) \end{bmatrix} \tag{38}$$

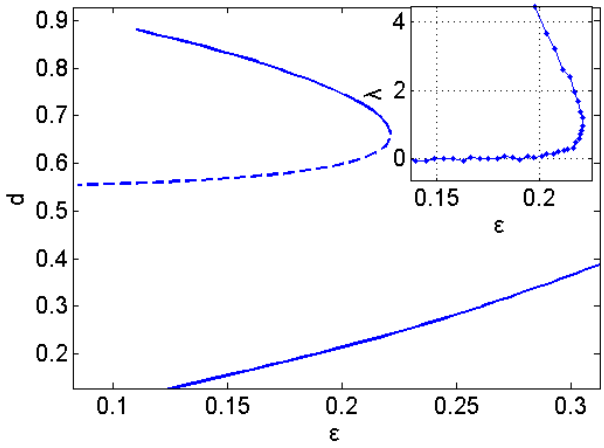

Figure 6: Coarse-grained bifurcation diagram of the density of "A" voters with respect to the switching probability ε, using the detailed majority-voter simulator evolving on an Erdös-Rényi network constructed with connectivity probability $p = 0.0008$, adding, self connection for each node. Solid lines correspond to the coarse-grained stable states while the dotted lines correspond to unstable ones. The inset depicts the computed eigenvalue λ, determining the systems, coarse grained stability.

Note that for the calculation of the Jacobian $\frac{\partial \Phi_T}{\partial d}$ and $\frac{\partial \Phi_T}{\partial \varepsilon}$, no explicit macroscopic evaluation equation are needed. They can be approximated numerically by calling the black-box coarse timestepper at appropriately perturbed values of the corresponding unknowns (d, ε). The above framework enables the microscopic simulator to converge to both coarse-grained stable and unstable solutions and trace their locations [25]. The eigenvalues (here is just one) of the Jacobian $\frac{\partial \Phi_T}{\partial d}$ determine the local stability of the stationary solutions: a fixed point is stable when the modulus of all eigenvalues is smaller than one and unstable if there exists at least one eigenvalue with modulus greater than one.

Each bifurcation diagram consists of two families of solutions. One family of solutions is characterized by a saddle node bifurcation: the high density state (where the majority of individuals vote for A) bifurcates through a turning point (found at $\varepsilon = 0.2207$, $\varepsilon = 0.1869$ and $\varepsilon = 0.1641$, for the networks of ER (Fig. 6), WS (Fig.7) and Barabasi (Fig.8) respectively), marking the change in the stability. The second family of low density states (where the majority of B voters), is stable for all values of ε for all the networks.

In Figs. 9, 10 we also show the bifurcation diagrams obtained using the mean field approximations as these are derived from Eq.(30),(31) and (33) using the ER and WS degree distributions respectively. The degree distributions are taken to be symmetric around $k = 8$.

The coarse-grained bifurcation diagrams obtained using the detailed individual-based model evolving on the ER and WS networks are also shown for comparison reasons. The relatively simple mean field models assume randomly selected individuals with replacement, omitting therefore spatial correlations. Compared to the results obtained by the Equation-free approach, the MF approximation in the case of the ER networks gives

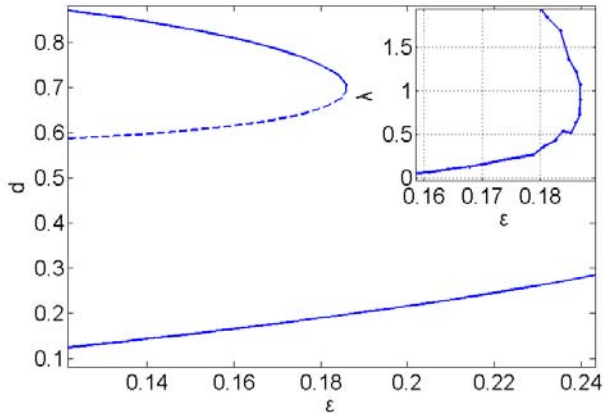

Figure 7: Coarse-grained bifurcation diagram of the density of "A" voters with respect to the switching probability ε, using the detailed majority-voter dynamics simulator evolving on a WS network constructed with rewiring probability $p = 0.2$ and $2k = 8$ initial neighbors, adding self connection for each node. Solid lines correspond to the coarse-grained stable states while the dotted lines correspond to unstable ones. The inset depicts the computed eigenvalue λ, determining the systems, coarse grained stability.

almost identical bifurcation diagrams. In the case of WS the MF gives a qualitatively similar bifurcation diagram, yet a quantitatively different one. In particular, close to the coarse-grained criticalities, the analytical model deviates from the actual detailed simulation results, while the Equation-free framework captures the correct coarse-grained behavior.

7 Conclusions

Over the years, majority-rule or as otherwise called majority-voter models have been extensively used to gain a better understanding on the behavior of many complex systems as diverse as opinion formation and voter/election dynamics, epidemic spread dynamics, culture and language dynamics, crowd flow design and management, and neuroscience. Due to the nonlinear, stochastic nature of such individualistic models and their coupling to complex network structures, the emergent behavior cannot be-most of the times-accurately modeled and analyzed in an efficient straightforward manner. Hence, the systematic exploration of the emergent dynamics of network-evolving individualistic models and in particular those based on the majority-rule mechanism becomes, in this context, of great importance. We proved analytically how the parity and heterogeneity of the degree distributions influences the symmetry of the coarse-grained stationary solutions of the basic majority-voter model.We constructed the mean field approximations of the majority-voter dynamics describing the evolution of the zero-th order moment of the underlying distributions (that is the density of A voters). We also showed how one can exploit the Equation-free framework to bridge the micro to macro scales of the dynamics of stochastic individual-based models that evolve on heterogeneous complex random graphs.

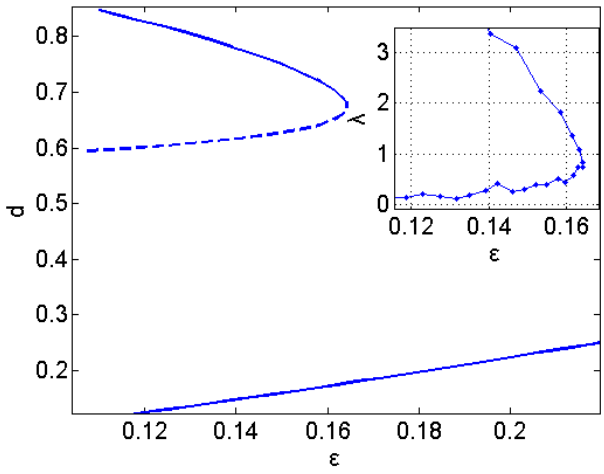

Figure 8: Coarse-grained bifurcation diagram of the density of "A" voters with respect to the switching probability ε, using the detailed majority-voter dynamics simulator evolving on a Barabasi network constructed with $m_0 = 3$ and $m = 2$. Solid lines correspond to the coarse-grained stable states while the dotted lines correspond to unstable ones. The inset depicts the computed eigenvalue λ, determining the systems, coarse-grained stability.

In particular, we showed how systems-level tasks such as bifurcation and stability analysis of the coarse-grained dynamics with respect to network topological characteristics can be performed bypassing the need to extract macroscopic models in a closed form. Our analysis was focused on four of most-cited types of complex networks: Random Regular, ErdsRnyi, Watts and Strogatz and Barabasi (scale free) networks. Using the individualistic, stochastic simulator as a black-box timestepper for the coarse-grained variables, we constructed the coarse-grained bifurcation diagrams with respect to the basic parameter of the majority-voter model: the switching state probability. The derived coarse-grained bifurcation diagrams were compared with the ones obtained using the corresponding mean field approximations. The analysis revealed that especially near the critical turning points the mean-field approximations introduce certain quantitative bias. However the efficiency of the Equation-free approach emerges in the case of scale-free networks. Due to the high heterogeneity of such networks with respect to the heavy tailed connectivity distribution, the bifurcation computations, based on the corresponding mean field approximation, become, as we discussed in section 4, an overwhelming difficult computational task. Further research could be directed towards the investigation of the influence of more accurate closures, such as the ones relating the correlations between the states of two or more connected nodes in the network leading to pairwise approximations [26, 27, 28, 46]. Another issue that could be also further studied is related to one of the basic prerequisites of the Equation-free framework: the a-priori knowledge of the appropriate observables. However, for arbitrary complex networks these are not known before-hand. In this case, the use of state-of-the-art data nonlinear dimensionality reduction techniques that can be exploited to efficiently extract the correct coarse-grained variables from a more complex individual-based large-scale code could be also attempted.

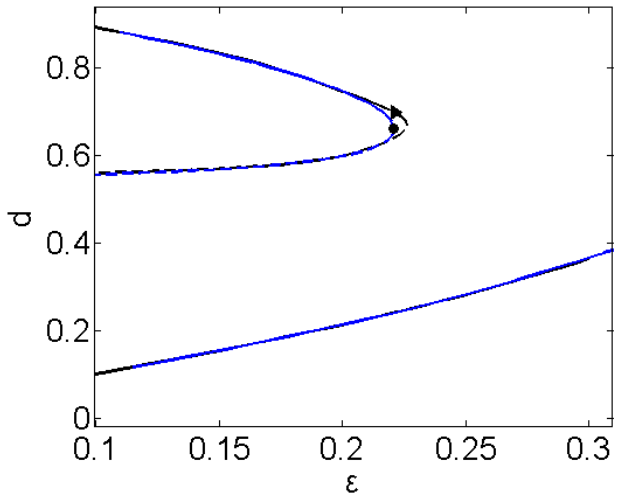

Figure 9: Bifurcation diagram of the density of "A" voters with respect to the switching probability ε, as obtained with the mean-field approximation of the majority-voter dynamics evolving on a Erdös Rényi type network with(marked with a triangle) compared to the coarse-grained bifurcation diagram obtained with the detailed simulator (marked with a circle).

References

[1] R, Albert and A. L, Barabasi, "Statistical mechanics of complex networks," Reviews of Modern Physics, 74, 47-97, 2002.

[2] E, Altshuler, I, Ramos, Y, Nunez, J, Fernandez, A. J, Batista-Leyva and C, Noda, "Symmetry Breaking in Escaping Ants," The American Naturalist, 166(6), 643-649, 2005.

[3] R, Axelrod, *The Complexity of Cooperation*, Princeton University Press, 1997.

[4] M, Boguná and R, Pastor-Satorras, "Epidemic spreading in correlated complex networks," Phys. Rev. E, 66, 047104, 2002.

[5] M, Boots and A, Sasaki, "'Small worlds'and the evolution of virulence: infection occurs locally and at a distance," Proc. R. Soc. Lond. B, 266, 1933-1938, 1999.

[6] C, Castellano, S, Fortunato and V, Loreto, "Statistical physics of social dynamics," Rev Mod Phys.,81, 591-646, 2009.

[7] C, Castellano, M, Marsili and A, Vespignani, "Nonequilibrium phase transition in a model for social influence," Phys. Rev. Lett., 85, 3536-3539, 2000.

[8] P, Clifford and A, Sudbury, "A model for spatial conflict," Biometrika, 60, 581-588, 1973.

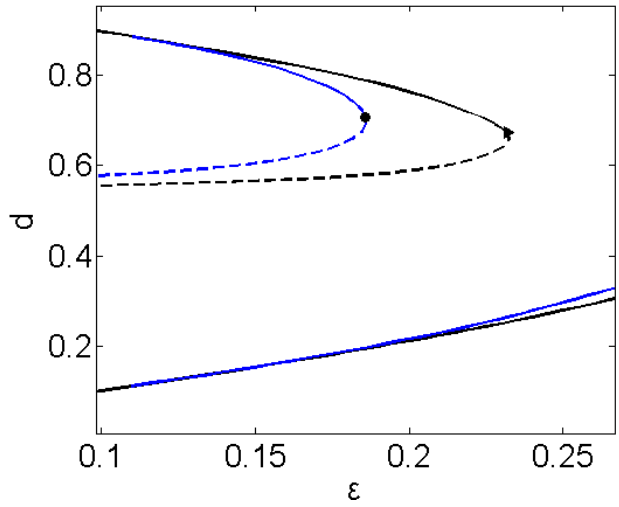

Figure 10: Bifurcation diagram of the density of "A" voters with respect to the switching probability, as obtained with the "mean-field" approximation of the majority-voter dynamics evolving on a WS type network with (marked with a triangle) compared to the coarse-grained bifurcation diagram obtained with the detailed simulator (marked with a circle).

[9] R, Cohen and S, Havlin, "Scale-Free Networks Are Ultrasmall," Phys. Rev. Lett., 90, 058701, 2003.

[10] S. N, Dorogovtsev and J. F. F, Mendes, "Language as an evolving word web," Proc. Roy. Soc. London Ser. B, 268, 2603-2606, 2001.

[11] M, Dungey, R, Fry, B. G, Hermosillo and V, Martin, "Contagion in international bond markets during the Russian and the LTCM crises," Journal of Financial Stability, 2, 1-27, 2006.

[12] P, Erdös and A, Rényi, "On random graph," Publicationes Mathematicae,6, 290-297, 1995.

[13] S. H, Eubank, V. S. A, Guclu, M, Kumar, M. V, Marathe, A, Srinivasan, Z, Toroczkai and N, Wang, "Modelling disease outbreaks in realistic urban social networks," Nature, 429, 180-184, 2004.

[14] C. W, Gear, I. G, Kevrekidis and C, Theodoropoulos "Coarse Integration/Bifurcation Analysis via Microscopic Simulators: micro-Galerkin methods," Computers and Chemical Engineering, 26, 941-963, 2002.

[15] X, Guardiola, A, Diaz-Guilera, C. J, Perez, A, Arenas and M, Llas, "Modelling diffusion of innovations in a social network," Phys. Rev. E, 66, 026121, 2002.

[16] H. A, Haveman, "Follow the leader: Mimetic isomorphism and entry into new markets," Administrative Science Quarterly, 38, 593-627, 1993.

[17] D, Helbing, I, Farkas and T, Vicsek,"Simulating dynamical features of escape panic," Nature, 407, 487-490, 2000.

[18] D, Helbing and P, Molnár, "Social force model for pedestrian dynamics," Phys. Rev. E, 51, 4282-4286, 1995.

[19] R, Holley and T, Liggett, "Ergodic theorems for weakly interacting infinite systems and the voter model," Ann. Probab., 3, 643-663, 1975.

[20] M. T, Hon, J. K, Strauss and S. K, Yong, "Deconstructing the Nasdaq bubble: A look at contagion across international stock markets," Int. Fin. Markets, Inst. and Money, 17, 213-230, 2007.

[21] R. L, Hughes, "The flow of large crowds of pedestrians," Math. Comp. Simul., 53, 367-370, 2000.

[22] A, Ianni and V, Corradi, "The dynamics of public opinions under majority rules," Review of Economic Design, 7(3), 257-277, 2002.

[23] A, Johansen, "Origin of crashes in three US stock markets: shocks and bubbles," Physica A, 338, 135-142, 2004.

[24] M, Joron and J, Mallet, "Diversity in mimicry: paradox or paradigm?," Trends in Ecology and Evolution, 13, 461-466, 1998.

[25] M, Kavousanakis, L, Russo, C. I, Siettos, A. G, Boudouvis and G. C, Georgiou,"A Timestepper Approach for the Systematic Bifurcation and Stability Analysis of Polymer Extrusion Dynamics," J. Non-Newtonian Fluid Mechanics, 151, 59-68, 2008.

[26] M. J, Keeling, "The effects of local spatial structure on epidemiological invasions," Proc. Roy. Soc. Lond.B, 266, 859-869, 1999.

[27] M. J, Keeling, "Implications of network structure for epidemic dynamics," Theor. Popul. Biol., 67, 1-8, 2005.

[28] M. J, Keeling and K. T. D, Eames, "Networks and epidemic models," J. R. Soc.Interface, 2, 295-307, 2005.

[29] I. G, Kevrekidis, C. W, Gear, J. M, Hyman, P. G, Kevrekidis, O, Runborg and C, Theodoropoulos,"Equation-free coarse-grained multiscale computation: enabling microscopic simulators to perform system-level tasks," Comm. Math. Sciences, 1, 715-762, 2003.

[30] I. G, Kevrekidis, C. W, Gear and G, Hummer, "Equation-free: the computer-assisted analysis of complex, multiscale systems," AI.Ch.E Journal, 50, 1254-1346, 2004.

[31] R, Kozma, M, Puljic, P, Balister, B, Bollobas, and W. J, Freeman, "Phase Transitions in the Neuropercolation Model of Neural Populations with Mixed Local and Non-Local Interactions, " Biol. Cybern., 92, 367-374, 2005.

[32] R, Lambiotte, M, Ausloos and J. A, Holyst, "Majority model on a network with communities," Phys. Rev. E, 75, 030101, 2007.

[33] R, Lambiotte, S, Thurner and R, Hanel, "Unanimity Rule on networks," Phys. Rev. E, 76, 046101, 2007.

[34] M, Llas, P. M, Gleiser, J. M, Lopez and A, Diaz-Guilera, "Nonequilibrium phase transition in a model for the propagation of innovations among economic agents," Phys. Rev. E, 68, 066101, 2003.

[35] V, Loreto and L, Steels, "Social dynamics: Emergence of language," Nature Physics, 3, 758-760, 2007.

[36] A, Makeev, D, Maroudas. and I. G, Kevrekidis, "Coarse stability and bifurcation analysis using stochastic simulators: Kinetic Monte Carlo examples," Journal of Chemical Physics, 116, 10083-10091, 2002.

[37] A. Melberg, *Theories of Mimesis*, Cambridge University Press, 1995.

[38] M. E. J, Newman, "The structure and function of complex networks," SIAM Review, 45(2), 167-256, 2003.

[39] A, Orlean, "Mimetic contagion and speculative bubbles," Theory and Decision, 27, 63-92, 1989.

[40] D. R, Parisi and C. O, Dorso, "Microscopic Dynamics of Pedestrian Evacuation," Physica A, 34, 606-618, 2005.

[41] J. M, Pacheco, F. L, Pinheiro and F. C, Santos, "Population structure induces a symmetry breaking favoring the emergence of cooperation," PLoS Comput Biol, 5(12), 1000596, 2009.

[42] A. I, Reppas, A. C, Tsoumanis and C. I, Siettos, "Coarse-Grained Bifurcation analysis and Detection of Criticalities of an Individual-Based Epidemiological Network Model with Infection Control," Applied Mathematical Modelling, 34, 552-560, 2010.

[43] O, Runborg, C, Theodoropoulos and I. G, Kevrekidis, "Effective bifurcation analysis: a timestepper-based approach," Nonlinearity, 15, 491-511, 2002.

[44] C. I, Siettos, M, Graham and I. G, Kevrekidis, "Coarse Brownian dynamics for nematic liquid crystals: bifurcation diagrams via stochastic simulation," Journal of Chemical Physics, 118, 10149-10156, 2003.

[45] D, Sornette and W. X, Zhoua, "Evidence of fueling of the 2000 new economy bubble by foreign capital infow: implications for the future of the US economy and its stock market," Physica A, 332, 412-440, 2004.

[46] K. G, Spiliotis and C. I, Siettos, "Computations on Neural Networks: from the Individual Neuron Interactions to the Macroscopic-level Analysis," Int.J.Bifurcation and Chaos, 20, 121-134, 2010.

[47] K. G, Spiliotis and C. I, Siettos, "A Timestepper-based Approach for the Systems-Level Analysis of Microscopic Neuronal Simulators on Networks: Bifurcation and Rare-Events Micro to Macro Computations," Neurocomputing, 74, 3576-3589, 2011.

[48] C. J, Tessone and R, Toral, "System size stochastic resonance in a model for opinion formation," Physica A, 351, 106-116, 2005.

[49] R, Topol, "Bubbles and volatility of stock prices: effect of mimetic contagion," Economic Journal, 101, 786-800, 1991.

[50] J, Watts and S. H, Strogatz, "Collective dynamics of 'small-world' networks," Nature, 393(6684), 440-442, 1998.

[51] F, Wu and B. A, Huberman, "Novelty and collective attention," PNAS, 104, 17599-17601, 2007.

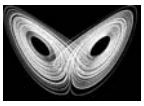

Annual Review of Chaos Theory, Bifurcations and Dynamical Systems
Vol. 2, (2012) 21-31, www.arctbds.com.

Convergent Numerical Solutions of Unsteady Problems

Lun-Shin Yao
School for Engineering of Matter, Transport and Energy
Arizona State University, Tempe, AZ 85287
e-mail: lsyao@yahoo.com

Abstract

Von Neumann established that discretized algebraic equations must be consistent with the differential equations, and must be *stable* in order to obtain convergent numerical solutions for the given differential equations. The "stability" is required to satisfactorily approximate a differential derivative by its discretized form, such as a finite-difference scheme, in order to compute in computers. His criterion is the necessary and sufficient condition only for steady or equilibrium problems. It is also a necessary condition, but not a sufficient condition for unsteady transient problems; additional care is required to ensure the accuracy of unsteady solutions.

Keywords: convergent numerical solutions, unsteady problems, stability.

Manuscript accepted April 10, 2012.

1 Introduction

Systems of ordinary differential equations that exhibit chaotic responses have yet to be correctly integrated. So far no convergent computational results have ever been determined for chaotic differential equations, since the truncation errors introduced by discretized numerical methods are amplified for *unstable* computations. Numerical methods usually convert continuous differential equations to a set of algebraic equations to be solved by computers. Von Neumann established that discretized algebraic equations must be *consistent* with the differential equations, and must be *stable* in order to obtain convergent numerical solutions for the given differential equations. A typical property of chaotic differential equations is that they are *unstable*. It is not straightforward to check the consistence and stability of a numerical computation. In particular, it lacks a practical

way to conveniently check the convergence of numerical results for *non-linear* differential equations that a linear stability analysis may not yield desirable and confident conclusions.

Parker and Chua [1] suggested a practical way of judging the accuracy of the numerical results from a non-linear dynamical system is to use two or more different methods to solve the same problem. If the two solutions agree then they can be assumed accurate. Viana [2] proposed to solve the same problem in two or more different machines to ensure the convergent results. Both approaches are testing to ensure that truncation errors will not overwhelm the correct solutions. The same propose can be achieved by solving the problem in one machine and one method, but two different integration time steps [3, 4]. All three ways are easy to apply, but the agreement of two computational results by either of these ways is only a necessary condition, and is not *sufficient*. Typical examples, well known to all graduate students in thermal science, are unsteady heat conduction problems; even though, the heat equation is linear. They demonstrated the additional difficult of checking convergence for unsteady problems.

Without knowing it is not a sufficient condition, Lorenz [5] mistakenly concluded that his solution for his 1990 model was convergent initially for thirty years! This contradicts to the fact that the initial period of the Lorenz solution for his 1990 model is mixed with many *unstable and divergent* sections with some stable sections. One cannot claim that the mixture of errors in many unstable computations with some short time convergent computations is a correct solution, since the differential directives cannot be replaced by their computable discretized forms unstable periods. We will explain why the convenient ways to check convergence of unsteady computation is insufficient below and followed by numerical examples.

2 Mathematical Explanation

We will solve a set of, or a differential equation

$$\frac{du}{dt} = f(u, t) \tag{1}$$

whose exact solution is $u = u(t)$. Let's use $X_i(t)$ $(i = 1, 2)$ denotes the computational results for two different methods, or two different machines, or two different integration time steps; $E_i(t)$ is the corresponding computational errors. Therefore,

$$X_i(t) = u(t) + E_i(t) \tag{2}$$

If the difference of two computational results is small, such as

$$|X_1 - X_2| = |E_1 - E_2| < \varepsilon, \tag{3}$$

where ε is a pre-assigned small number, it has a possibility that E_1 and E_2 are both small, and the computational results are convergent. On the other hand, (3) does not guarantee that both E's are small; it only states that the difference of two errors is small. Hence, (3) can only be a necessary condition. This is the mistake made by Lorenz [5].

3 Numerical Examples

Two examples will be given below to demonstrate the convergence of numerical solutions for differential equations.

A. The first one is a simple linear differential equation and we will construct stable computations to demonstrate that (3) is only a necessary condition.

The equation,

$$\frac{du}{dt} = -10u, \tag{4}$$

is used with the initial condition $u(0) = 1$. The exact solution is

$$u(t) = \exp(-10t), \tag{5}$$

The explicit finite-difference scheme is chosen for an unstable computation as

$$\frac{u^{n+1} - u^n}{\Delta t} = -10u^n$$

or

$$u^{n+1} = (1 - 10\Delta t)\, u^n. \tag{6}$$

It is clear that (6) is unstable, if $\Delta t > 0.1$, the truncation errors is $O(\Delta t)$. It is well known that the numerical result will diverge for an unstable computation. We will show two computational results in comparison with the exact solution: one is for $\Delta t = 0.05$; the other $\Delta t = 0.06$. Two computational results agree completely initially. This is because that the computations of first step for two different time steps are identical. Since the truncation errors are $O(\Delta t)$, the results for the first few steps, when the computation time is about the same $O(\Delta t)$, cannot be accurate. The comparison presented in the Fig. 1 demonstrates two computational results are not close to the exact solution even though they are fairly close to each other. This confirms the claim *that the small difference of two computational results can only be a necessary condition for the convergence of unsteady problems*. On the other hand, both computational results asymptotically converge to the exact solution, zero, for the steady problem. This is an example to show that von Neumann's consistent and stable conditions are necessary and sufficient for steady problems, but not sufficient for unsteady problems. For a *consistent* and *stable* computation, it still requires checking computed results by successively reducing time-step size until the difference is acceptably small; then, the convergence can be claimed [4] for an unsteady computation.

Another commonly known example, frequently taught in the first-year graduate course in heat transfer, is the heat equation. It is well known that a consistent and stable computation is sufficient to provide a convergent steady-state solution, but cannot guarantee a convergent transient solution. A convergent transient solution can only be obtained by successively reducing the integration time steps until the change of the computed transient results is acceptably small.

B. The second example is the Lorenz second model [4, 5, and 7]. The model is composed with three non-linear first-order differential equations.

$$\begin{cases} X' = -Y^2 - Z^2 - \frac{1}{4}(X - 8) \\ Y' = XY - 4XZ - Y + 1 \\ Z' = 4XY + XZ - Z \end{cases} \tag{7}$$

The initial condition used below is $(X = 2, Y = 1, Z = 0)$. The error curve presented in Fig. 2 is the difference of $X(t)$ computed by the fifth-order Taylor-series method [7] with 10-6 time step by the Taylor-series method for time-steps 10-7 , respective. The conclusion is independent of the numerical methods used to integrate the equations (7). The details of comparison of various methods can be found in [4].

The error curve shown in Fig. 2 differs obviously from any non-convergent error curves for any linear differential equations. The recorded difference of two computational results is too small when time is less than 30; so, we did not plot them. According to Lorenz's opinion [5], this shows that the numerical solutions are good for this short period of time; even thought, he agreed that numerical solutions for long time is not possible. It is worthy to point out that the time steps used in our computation is much smaller than what Lorenz used; so, our good results, according to Lorenz's criterion, can be extended to larger time. We will explain why this concept is wrong below.

The only available detailed error analysis for numerical solutions of non-linear differential equations, as we are aware, is for the famous Lorenz 1963 model [8]. It clearly demonstrated that two major amplification mechanisms exist for truncation errors, introduced by all numerical methods. The first is the explosive amplification mechanism, which can instantly amplify the truncation tremendously when the trajectory penetrates the separatrix by violating the differential equations. Since the Lorenz 1990 model does not have an attractor, the explosive amplification does not occur, confirmed by our numerical computations [4]. We will not further discuss it here; the interested readers can read [8].

The second mechanism is the exponential amplification of errors, which is also found in the numerical solution of linear differential equations as explaining in the first example. An unstable computation for unsteady linear differential equations can result two kinds of behaviors uniformly in time: exponential growth of errors, or exponential growth of the amplitude of oscillatory solutions. The crucial difference between non-linear differential equations and linear ones is the exponential error amplification for non-linear differential equations is not uniform in time, see Fig. 2. The growth of truncation errors occurs in "irregular valleys". This suggests the existence of certain dynamic structures in the phase space. This agrees with the *exponential amplification* of errors described in [8]. When two trajectories move along the direction of a stable manifold, the distance between them shrinks; in other words, errors are reduced; when trajectories move along an unstable manifold, errors are amplified. The combined consequence is, however, the exponential growth of truncation errors in time as shown in Fig. 2.

It should be emphasized here that the error amplification is due to the unstable computation locally, which violates von Neumann's convergence criterion. For linear differential equations, it will lead to divergent solutions; one would not expect it could provide correct solutions for non-linear differential equations. If it were so, it would mean that it were easier to numerical integrated non-linear differential equations, since no check of convergence would be needed. Then, it was always legitimate to replace a derivative by

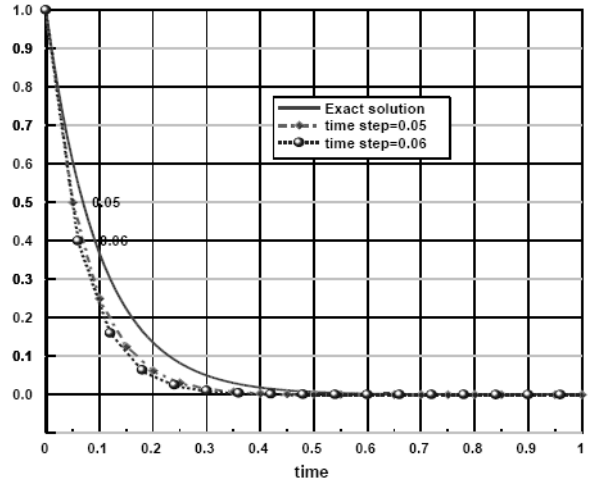

Figure 1: Comparison of computational results with the exact solution. The number on the right of the plotting points indicates the computational time of the point.

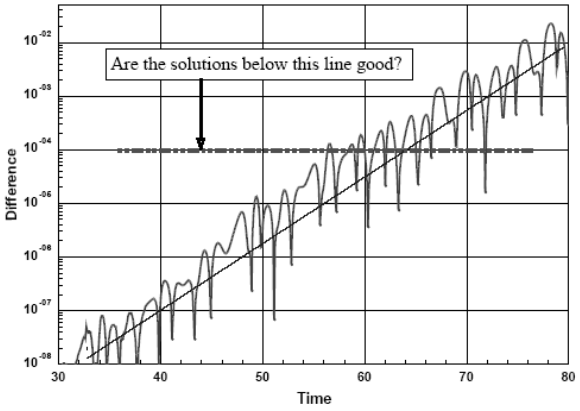

Figure 2: The difference of numerical results of time steps 10^{-6} and 10^{-7}.

a finite-difference counterpart without worrying they may not even be approximations! This is exactly what has happened in solving chaos or turbulence numerically now.

It is also worthy to mention that it has been demonstrated in [8] that a small difference of two computations does not imply either one is close to the correct solution for unsteady problems. This has been experienced many times in the history of numerically solving both linear and non-linear differential equations of unsteady problems, but has been overlooked in solving chaos or turbulence numerically.

This difficulty associated with unstable computation is the property of non-linear differential equations, and cannot be remedied by adjusting numerical methods, see [8]. Since the truncation errors are not controllable and occur randomly, the numerical computational chaos results, or turbulence is also random in nature; irrespectively, the associate boundary conditions are either independent of time, or depend on time regularly. Consequently, an unstable numerical result is the random amplification of truncation errors, induced by numerical processes, and has no physical meaning.

We do not believe that our paper can reverse the avalanche of treating numerical errors as numbers with physical significance, but hope someone, in the near future, may take a little effort to honestly compare computational results with carefully carry-out measurements. It is time to reconsider the activities of continuously producing numerical errors in large amount without any justification. Fundamental principles in science should always be respected before one can prove otherwise.

4 Comments, discussions, and open problems from some experts in the field

I will first outline some well-known basic principles in numerical mathematics, which will help to explain the following questions. In calculus, we know

$$\frac{\partial u}{\partial t} = \lim_{\Delta t \to 0} \frac{u\left(t + \Delta t\right) - u\left(t\right)}{\Delta t} \tag{8}$$

Since computers are digital computational devices, it is necessary to discretize a derivative in order to calculate it in computers. I will use a finite-difference scheme as an example below; the principle can be equally applied to all discretized numerical methods without exception. A derivative can usually be replace by a finite-difference form,

$$\frac{\partial u}{\partial t} = \left(\frac{u\left(t + \Delta t\right) - u\left(t\right)}{\Delta t}\right) + TE\left(\text{truncature errors}\right), \tag{9}$$

where TE represents truncation errors and is of $O\left(\Delta t\right)$ in the above example. In the limit of Δt approaches zero, (9) agrees with (8). The TE always exists in any discretized process. Algebraic equations are resulted after all derivative terms being replaced by their difference forms; for example, terms in the bracket in (9). If the resulting algebraic equations are *stable*, TE will be exponentially decayed and the term inside the bracket is a good approximate of the derivative, since (8) will be asymptotically satisfied. On the other hand, if the resulting equations are *unstable*, the TE will be exponentially growing, and (8) is violated, or it implies that

$$\frac{u\left(t + \Delta t\right) - u\left(t\right)}{\Delta t} \text{ does not converges to } \frac{\partial u}{\partial t}. \tag{10}$$

The resulting equations after discretization have nothing to do with the original differential equations, and certainly are not an approximation of the original differential equations. Thus, the solutions of such algebraic equations are unrelated to the original differential equations. For linear differential equations, an unstable computation usually results exponentially divergent results, or exponentially divergent oscillatory results, a clear sign of a failure computation. This is why von Neumann put forward that the "stability" is the necessary and sufficient condition for a convergent solution for *steady-state* problems.

For *unsteady* problems, it is necessary to use even smaller Δt than required the one by Courant-Fredrich-Levy (CFL) condition in order to get an accurate transient solution as demonstrated in the first example of the current paper. There are many examples can

be found in heat conduction problems in undergraduate heat transfer textbooks. Consequently, stability is only a necessary condition to obtain an accurate transient solution.

I will answer and discuss the following questions.

1. The author comments the stability of the numerical computations for nonlinear ordinary differential equations. More precisely, the author comments that the agreement of two computational/numerical results is only necessary not sufficient condition for the accuracy of the computational/numerical results. Really, the accuracy of the computational/numerical results is very important scientific problem. Unfortunately, the author doesn't propose a way for the solution of this problem.

Answer: The answer to this question is very simple for linear or non-linear differential equations, if the resulting algebraic equations are *stable*; continuously reducing the integration time step, Δt until the change of the transient solutions for two different time steps becomes acceptably small. Then, both results can be considered as an accurate transient solution. If one carries out the computation of the first example in the paper by further reducing the integration time step, an accurate transient solution can be readily found, and agree with the exact solution to any degree as one wish. There are many other examples of heat conduction problems can be found in undergraduate heat transfer texts.

For non-linear chaos differential equations, *when the governing parameter is larger than its critical value*, the situation becomes much more complex. Two Lorenz's models have been discussed in [4, 8] and his second model is also used as the second example of this paper. The Lorenz's first model was analyzed in detail and reported in [8]. It shows that the truncation (numerical) errors are amplified exponentially in the unstable region (manifold); are reduced exponentially in the stable region (manifold). According to the basic principle outlined above, it is clear that the numerical results in the unstable regions cannot be considered as an approximate solution to the original differential equations. Similar conclusion can be made for the Lorenz's second model and reported in [4].

In addition, we have identified that the Lorenz's first model contains local separatrix, not in his second model. The truncation errors can be amplified explosively when the trajectory penetrates the virtual separatrix, which violates the differential equations. The existence of a virtual separatrix is a consequence of singular points of a non-hyperbolic system of differential equations, which is not *shadowable* [8, 9]. A commonly cited computational example in chaos involving two solutions of slightly different initial conditions that remain "close" for some time interval and then diverge abruptly when one penetrates the virtual separatrix, violating the differential equations and the other does not. Before it was pointed out in [8, 9], that this phenomenon is actually due to the explosive amplification of numerical errors, and violation of the differential equations as described above, this behavior was often believed to be a *typical characteristic of chaos*, and frequently used as the evidence that a computation is chaos. Similar computational results can occur for two different integration time steps; many would consider such results as acceptable since it is a "twin brother" of sensitivity to initial conditions and a typical characteristic of chaos. This mistake deserves clarification and explained thoroughly in [8].

Additional examples for other non-linear chaos differential equations are cited in [3]. The central issue discussed in [9] is that no chaos solution exists for differential equations,

since all computations are unstable. This is the obvious consequence that all discretized numerical methods have truncation errors and are incapable to solve chaos differential equations.

Since non-linear differential equations can have *multiple solutions* when the value of its parameter is larger than its critical value, once the trajectory went in the unstable region, the amplified truncation errors alters its initial condition equivalently for the next stable region. This can lead to next stable solution from the one that one was originally trying to get as discussed in [10]. This is a brand new topic, which has never been studied, yet.

2 I tried to re-evaluate the revised version of the manuscript in goodwill. However in his revised manuscript the author insists in keeping his claim that "Lorenz [5] mistakenly concluded that his solution for his 1990 model was convergent initially for thirty years!" (in Introduction). For me this was the one and only major issue I had, as reading Lorenz's answer to Yao and Hughes published in Tellus (2008), 60A, 806–807, I think that this claim is both strong and wrong.

Answer: The answer of this question is simple and clear by judging it from the basic principle outlined above. Lorenz's numerical results of his second model clearly show the trajectory went through stable and unstable regions alternatively, see Fig. 2 of the paper and [4]. The difference of the results for two different time steps increases when the trajectory moves in the unstable region, where (8) is violated; the difference decreases when the trajectory moves in the stable region. Can one claim such a computational result is good when most parts of it violate (8), a definition in calculus?

Many authors followed Lorenz's step [14] and claimed mistakenly that their solution is good for a short initial period. Form the above discussion; it is clear that the initial good period will be zero, if the initial point is selected in the unstable region. If the initial condition is located in the stable region, the computed result will be good until it moves out of the stable region and gets into the unstable region.

Since without numerical instability, there is no chaos; so they can only claim their results is a good regular solution, not chaos for the initial period. I want to emphasize again that all numerical chaos are amplified numerical errors.

3 The topic of this paper is rather interesting. But the extension and scope of the paper seems to be very brief for what such a topic may require. The references seem to be devoted to self-citations, when there is a huge amount of scientific literature in the field.

Answer: Detailed analysis are available in [3, 4, 8, 9] and additional references are listed below, which are all my own work. I do not know the existence of any written paper in line with my conclusion. If there are some, I welcome readers to reveal them to me. The entire huge amount of scientific literature devotes to treat amplified numerical errors as computed chaos with very few exceptions cited in the additional references listed below. This is exact the reason that I tried to push this paper forward. Fortunately, science is not a democratic system that majority wins; in fact, truth always prevails in science. I hope the basic principles, outline above, can help readers to analyze the situation rationally by themselves, not just follow the argument of established authorities.

4 The major part of the discussion seems to be devoted to demonstrate "that the small difference of two computational results can only be a necessary condition for the convergence of unsteady problems". All the discussion seems to emerge from Eq. 3, which from another side (may be a too simplistic one), seems to be self-evident: "getting two bad results rather similar does not guarantee that the conclusion is alright". The focus of the discussion could be set in dealing with the definition of good or bad.

Answer: I do not really understand this question, but I believe the above discussion has already answered this question.

5 It may be of interest to cite some of the large amount of references in the literature devoted to the topic of solving a problem by computing many similar initial conditions/parameters, and analyzing later the results. This aims to assign given probabilities of success to every computed solution (as for instance in the field of meteorology).

Answer: Please read the answer of the second question, and note that the large amount literatures ignored the basic principles discussed above.

I would like to point out that a slightly different initial condition can result a completely different long-time solution for non-linear differential equations when the governing parameter is above its critical value; so there are multiple solutions exists even for non-turbulent flows. I list some references [11-14] below for interesting readers to explore. More references can be found in them. They are also all my works, since my works are the only theoretical studies exist, beside few experiments in fluid mechanics.

It is worthy to mention, from our experience, that the computation of the Navier-Stokes equations fails to converge if the Reynolds number is too much larger than the critical Reynolds number. This is the reason why a direct numerical simulation cannot be use to study flow transition; so, it is also unhelpful for turbulence.

A well-known excise to stabilize an unstable computation is to use upwind difference scheme; however, the added *numerical viscosity* associated with the upwind difference scheme may overwhelm the actual viscosity to invalidate the computational results. One can see why weather forecast is so unreliable, it is not because that the Navier-Stokes equations are incorrect; it is due to lack of a method to solve them correctly.

6 Along the paper, the concepts of chaoticity and stability seem to be mixed somehow, and a clear separation of both definitions should be appreciated.

Answer: The rigorous mathematical definition of chaos can be found in [2, 8].

Traditionally, the linear stability analysis in fluid dynamics is to study the growth or the decay of a very small perturbation quantity added to the steady-state base flows. For a laminar flow, the differential equations are stable, but the difference scheme can be unstable. This leads to CFL condition.

The extension of such analysis for time-dependent base flows is complex and unsuccessful. The linear-stability analysis of the algebraic equations resulted from the discretization of differential equations is very similar to the stability analysis in fluid dynamics. An easy

alternative is to solve differential equations with two different time steps, and hope the difference is acceptably small as discussed in this paper.

For chaos differential equations, it becomes very complex, since the differential equations are themselves unstable. There is no way to design a stable numerical method for unstable differential equations. As noted in the Question 5, there is a well-known way to stabilize an unstable computation by using use upwind difference scheme; however, the added *numerical* viscosity associated with the upwind difference scheme may overwhelm the actual viscosity to invalidate the computational results.

I have repeatedly tried to explain that numerical chaos is simply amplified numerical errors. Numerical chaos and numerical instabilities are different titles, but the same object.

7 The last paragraph on page 6 deals with the numerical computational chaos results. I agree with the fact that any numerical scheme will diverge from a true orbit beyond certain timescales for given problems. But some discussion about how these timescales may vary depending on the nature of the orbit, and even may be very long even when the orbit is chaotic is of interest. A discussion about the shadowing and predictability topics should be also appreciated.

Answer: This answer of this question is a part of the Question 2 and copy below for the convenience of readers.

Many authors followed Lorenz's step [5] and claimed mistakenly that their solution is good for a short initial period. Form the above discussion; it is clear that the initial good period will be zero, if the initial point is located in the unstable region. If the initial condition is selected in the stable region, the computed result would be *good* until it moves out of the stable region and gets into the unstable region.

The concept of shadowing is briefly reviewed in [9]. It was originally invented to save chaos theories for the hyperbolic systems. Since the relation between chaos theory and differential equations has not been established (Smale's 14th problem) and topological transitivity cannot be proved and is likely invalid, shadowing is not a useful concept for differential equations.

8 There is a vast amount of literature devoted to the numerical methods and how they deal with chaos. A brief panorama of the field should be of interest. After this, it may happen the statement "but hope someone, in the near future, may take a little effort to honestly compare computational results with carefully carry-out measurements" should be revised by the author.

Answer: It is a fact there is a large amount of literature devoted to the numerical methods and chaos, since both are the main streams of research in their areas and have been heavily funded by government agents; in particular, in the US. How could so many smart researchers all made the same mistake of violating the basic principles of numerical methods in solving differential equations, put forward by von Neumann?

Maybe, this is due to the limitation of human brains to discover brand new idea; instead, we look established authorities for guidance. However, please read my answer of the question 3 above.

References

[1] T. S, Parker & L. O, Chua, "Practical Numerical Algorithms for Chaotic Systems," Springer, 1989.

[2] M, Viana, "What's new on Lorenz strange attractors?" The Mathematical Intelligencer, 22, 6-19, 2000.

[3] L. S, Yao. "Is a Direct Numerical Simulation of Chaos Possible? A Study of a Model Non-Linearity," International Journal of Heat and Mass Transfer, 50, 2200–2207, 2007.

[4] L. S, Yao & D, Hughes, "A comment on "Computational periodicity as observed in a simple system," by Edward N. Lorenz (2006a), Tellus 60A, 4, 803-805, 2008.

[5] E. N, Lorenz, "Reply to comment by L.-S. Yao and D. Hughes," Tellus, 60A, 806–807, 2008.

[6] E. N, Lorenz, "Deterministic Nonperiodic Flow," Journal of the Atmospheric Sciences, 20, 130-141, 1963.

[7] E. N, Lorenz, "Can Chaos and Intransitivity lead to Interannual Variability?" Tellus, 42A, 378-389, 1990.

[8] L. S, Yao, "Computed Chaos or Numerical Errors," Nonlinear Analysis: Modeling and Control, 15(1), 109-126, 2010.

[9] L. S, Yao. "Nonexistence of Chaotic Solutions of Nonlinear Differential Equations," in "Frontiers in the study of chaotic dynamical systems with open problems" (Z.Elhadj & J.C.Sprott) (Eds), WORLD SCIENTIFIC SERIES ON NONLINEAR SCIENCE, SERIES B, 16, 31-41, 2010. [http://www.worldscibooks.com/chaos/8089.html]

[10] L. S, Yao, "Non-linear Instabilities," Chapter 6 in "Advanced Topics in Nonlinear Chaotic Systems," LAP LAMBERT Academic Publishing, http://www.lappublishing.com, ISBN-13:978-3-8465-8624-2, 127-140, 2012.

[11] L. S, Yao & S. G, Moulic, "Uncertainty of convection," Int. J. Heat & Mass Transfer, 37, 1713-1721, 1994.

[12] S. G, Moulic & L. S, Yao "Taylor-Couette instability of traveling waves with a continuous spectrum," J. Fluid Mech., 324, 181-198, 1996.

[13] L. S, Yao, "A resonant wave theory," J. Fluid Mech, 395, 237-251, 1999.

[14] L. S, Yao, "Multiple solutions in fluid mechanics," Nonlinear Analysis: Modelling and Control, 14(2), 263–279, 2009.

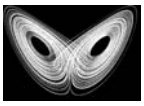

Annual Review of Chaos Theory, Bifurcations and Dynamical Systems
Vol. 2, (2012) 32-54, www.arctbds.com.

Nonlinear Control and Chaotic Vibrations of Perturbed Trajectories of Manipulators

Przemyslaw Szumiński
Technical University of Lodz, Stefanowskiego 1/15, 90-924 Lodz, Poland
e-mail: Przemyslaw.Szuminski@lodz.pl.

Tomasz Kapitaniak
Technical University of Lodz, Stefanowskiego 1/15, 90-924 Lodz, Poland
e-mail: Tomasz.Kapitaniak@lodz.pl.

Abstract

We study different types of manipulators' attractors and propose a motion control method. In our analysis the manipulator's motion is perturbed and its stability investigated using the nonlinear equations of perturbations and linearized equations for practical control. In order to realize a practical control the common areas of stability for nonlinear and linear models are identified. The maps of stability calculated as functions of model parameters are proposed as a tool for motion control. The spectrum of Lyapunov exponents is introduced as a practical measure of motion quality. The procedure allows choosing a way of reaching system stability in order to avoid undesired attractors. Additionally, the possibility of the occurrence of strange chaotic attractors in manipulators, ways they appear, and codimension 2 bifurcations have been analyzed.

Keywords: Nonlinear vibrations, stability, Lyapunov exponents, manipulator.

Manuscript accepted June 20, 2012.

1 Introduction

The problems concerning mechanical vibrations of manipulators create an important issue in the manipulator design and its motion control. Numerous papers devoted to mechanical vibrations attempt answering the question, if and when vibrations of manipulator links occur during its motion [12-36]. These considered both, the theoretical and practical

aspects respectively, through investigations of single links, with a special emphasis on their flexibility for example [24-38]. Such methods have been usually based on classical equations of dynamics [20], most often in the form of equations of control [9-29-13].

The theory of nonlinear dynamics provides new possibilities of analysis of the dynamics and control of mechanical systems. The investigations that have been conducted allowing studies of new types of behavior in simple mechanical systems, such as vibrating oscillators by means of theory of bifurcations [16-43], spectrum of Lyapunov exponents, Poincaré maps [3-18]. In mechanical systems, chaos may lead to irregular operations and fatigue failure [8-25-31]. From this point of view the control of chaos is understood as a way to stabilize an unstable motion. Many papers show different ways of analysis of control in the case of nonlinear dynamics of manipulators. For example the papers by Caracciolo have proposed two control schemes that have been designed to achieve satisfactory performance in the position and vibration controlling of two closed-chain planar manipulators with flexible links. The control schemes have been designed, tuned and tested in simulation, where the dynamic behavior of the flexible manipulators have been reproduced through a fully coupled nonlinear model based on the finite element theory. The bifurcation control scheme may be implemented either with or without a feedback. In the latter case, we have the open-loop control. In static feedback control, the feedback is used to achieve desirable nonlinear dynamics when locations of equilibria are known [1-39]. When these locations are affected in the controlled system we can use dynamic feedback control [2-39]. In case of dynamic feedback control, it is possible to preserve the equilibrium positions in the controlled system.

In [4] the authors have examined open-loop control of chaotic dynamics of a nonlinear system by applying weakly periodic perturbations. One of the most popular approaches of chaos control is the method named Ott-Grebogi-Yorke (OGY) and proposed in [15-26]. In the OGY scheme, the control of chaos is understood as stabilization of unstable periodic orbits embedded in a chaotic attractor by application of appropriate small perturbations on a single system parameter. In order to achieve this task, the dynamics of the system is followed by analyze of the Poincaré map. The unstable point of periodic orbit on Poincaré map can be stabilized when the value of the modulus of the eigenvalues in the control matrix [26] is smaller than one. In the Pyragas method of chaos control [28], stabilizing of unstable periodic orbits has been applied by use of small time continuous control of a parameter of a system, while it evolves in continuously understood time. This method is known as delayed feedback control.

In [40] the authors have employed the time-delay feedback to anti-control of a permanent magnet DC (PMDC) motor system for vibratory compactors, and hence implement the new, electrically chaotic compactor. Firstly, the dynamic model of the anti-controlled PMDC motor system and the proposed electrically chaotic compactor have been formulated. Secondly, a nonlinear map have been derived in order to analyze the chaotic criterion of the anti-controlled PMDC motor system. Anti-control of chaos of single time scale brushless DC motor have been studied in [5]. Anti-control of chaos have been achieved by addition of an external nonlinear term. Then, by addition of some coupling terms, using the Lyapunov stability theorem and linearization of the error dynamics, the chaos synchronization between a third-order brushless DC motor and a second-order Duffing system have been presented. In the paper [23] a new technique of generating several independent

chaotic attractors by design a switching piecewise-constant controller in continuous-time systems has been shown. The controller can create chaos using an anti-control of chaos feedback. It has been shown that nonlinear continuous-time system can possess several attractors, depending on the initial conditions.

More detailed information about the stability analysis based on different assumptions can be found in [6-7-10-11-22-33-41].

The spectrum of Lyapunov exponents is a powerful tool of the analysis of the nonlinear system dynamics due to fact, its values easily illustrate exponential divergence or convergence of the trajectory on attractor [19]. The exponents describe logarithmic measure of the sensitivity of the dynamical system on arbitrary small changes in the initial conditions. Their computation is, however, time-consuming and generally complex for most of the nonlinear dynamical systems with more than one degree of freedom. Therefore, it is impossible directly employing this tool in the analysis of the motion. Some algorithms for calculation and mathematical description of Lyapunov exponents can be found in [17-18-19-25-42].

One of the reasons of limited use of nonlinear theories in technical applications is that, the numerical computations are often regarded as impractical. In the present paper, we suggest a method for the analysis of manipulator vibrations and nonlinear control based on the analysis of stability regions in the stability maps of the nonlinear and linearized system. The method allows controlling of the system in real time. Additionally, the presented method allows analyzing effects of changes of various parameters on the manipulator vibrations after a perturbation of its motion. We also propose a practical scheme of control, based on the so-called stability maps. The first step of the controlling method consists of the determination of critical values of manipulator's parameters for which a change in stability, i.e., a bifurcation, takes place. The idea of manipulator instability is understood as instability in the sense of Lyapunov [14-19]. Determining of the spectrum of Lyapunov exponents and the Poincaré maps have allowed successful investigation of asymptotic behaviour of the phase flow in the neighborhood of the trajectory after a perturbation. Then, nonlinear equations of the perturbations allow determination of the nonlinear regions of stability of the manipulator motion.

However, such a determination of requires exhaustive mathematical computations and cannot be used for control in practice. A linear stability of the manipulator is investigated by calculating, in real time, the eigenvalues of the Jacobian matrix in a close neighborhood of the perturbation point in the manipulator's nominal motion. As a result, the comparison of stability regions of the nonlinear and linearized systems allows determination of their common parts. For these subregions the ranges of system parameters corresponding to them are determined. The motion control is based on the selection of such control parameters for which the manipulator remains in the stability subregion. In practice, for the assumed ranges of perturbations, the stability subregions are stored in the control system memory in the form of a collection of maps. The actual measurements of perturbations allow for a practical selection of the control parameters from the collection (performed for assumed trajectory parameters). The determination of values of the parameters is ruled by a choice of the way the stability region is reached. It is connected with a specified bifurcation type, which takes place during the transition of the motion towards the stability region.

The advantage of the proposed method is a possibility of real-time motion control by analysis of nonlinear stability regions without any differentiation of the equations during the manipulator motion. Additionally, possibilities of occurrence of chaotic vibrations in the form of a strange chaotic attractor may be also investigated. The ways of a stability loss are investigated through the analysis of the bifurcation types [21-25-27-30-35-36-]. A theoretical analysis of nonlinear dynamics performed for the 7MAR manipulator is presented as an example.

2 Equations of perturbations, linear and nonlinear stability

The issue of stability of the motion becomes important when the gripping device motion becomes unstable for some parameters of the manipulator's model. Let us assume that the vector of the generalized coordinates of the links (the state vector) $\mathbf{q}(t,\varepsilon) = [q_{01}(t),\ldots,q_{0n}(t)]^T$, where n is a number of degrees of freedom of the links, is a solution to the autonomous equation of motion

$$\dot{\mathbf{q}} = \mathbf{F}(\mathbf{q},\varepsilon)\,, \tag{1}$$

where the state vector $\mathbf{q} \in R^{2n}$, the parameter vector $\varepsilon \in R^m$, Eq. (14), and the vector field $\mathbf{F}$ is defined for $R^{2n} \times R^m$. Let us perturb this solution. The vector of perturbation of the state vector has the form

$$\psi(t) = \mathbf{q}_p(t,\delta) - \mathbf{q}(t,\varepsilon)\,, \tag{2}$$

where $\varepsilon \in \delta$, δ is the vector of parameters of perturbation. A perturbation of motion of an arbitrary generalized coordinate can be described as

$$\psi_i(t) = q_{pi}(t,\delta) - q_{0i}(t,\varepsilon)\,, \tag{3}$$

where $\psi_i(t)$ describes a perturbation of the i-th generalized coordinate, $q_{pi}(t)$ is a perturbed motion of i-th generalized coordinate. The distance of the solution of the manipulator perturbed motion from the solution of the nominal motion is defined by $\mathbf{y}(t)$. Generally, the vector of perturbations which can appear during motion can be presented as

$$\mathbf{y} = \left[\psi_1, \dot{\psi}_1, \ldots, \psi_i, \dot{\psi}_i, \ldots, \psi_n, \dot{\psi}_n\right]^T . \tag{4}$$

Deflections of positions from the nominal motion and their time derivatives that appear in the mechanical system of the manipulator are compensated for by changes in values of the driving torques of the nominal motion. Let us write the vector of compensating driving quantities as

$$\boldsymbol{\Delta} = [\text{control system } 1,\ldots,\text{control system n}]^T . \tag{5}$$

The compensation vector $\boldsymbol{\Delta}$ is in practice a set of parameters of the control systems.

Substituting Eqs. (2) and (4), their derivatives and a vector of compensating quantities $\mathbf{\Delta}$ into the equations of motion, we obtain the dynamics equations of the perturbed motion

$$\dot{\mathbf{y}} = \mathbf{A}\mathbf{y} + \mathbf{B}\mathbf{\Delta} + \mathbf{N}\,, \tag{6}$$

where $\mathbf{y}$, $N \in R^{2n}$, $\mathbf{A}(\mathbf{q}, \dot{\mathbf{q}}, \ddot{\mathbf{q}}, \varepsilon) \in R^{2n\times 2n}$, $\mathbf{B}(\mathbf{q}) \in R^{2n\times n}$, $\mathbf{\Delta} \in R^n$. A Taylor series has been used to expand the trigonometric functions including components of the vector $\mathbf{y}$. A degree of nonlinearity of Eq. (6) depends on the form of the series expansion of the trigonometric functions. The matrix $\mathbf{N}(\mathbf{q}, \dot{\mathbf{q}}, \ddot{\mathbf{q}}, \mathbf{y})$ includes the nonlinear terms of the equations of motion (6). After the perturbation of the manipulator operation, its nominal motion has been eliminated from the perturbation equations due to the extraction of classical equations of dynamics of the nominal motion from them. Next, the equations of dynamics written for the nominal motion of the manipulator has been extracted from the perturbation equations, taking thus into consideration the manipulator's motion after perturbation. It is possible, due to the fact, the nominal motion is compensated for through the nominal driving torques of the drive systems. As a result Eq. (6) received the form

$$\dot{\mathbf{y}} = \mathbf{G}(\mathbf{y}, \mathbf{q}, \dot{\mathbf{q}}, \ddot{\mathbf{q}}, \varepsilon, \mathbf{\Delta})\,, \tag{7}$$

where $\mathbf{y} \in R^{2n}$, the parameter vector $\varepsilon \in R^m$, $\mathbf{\Delta} \in R^n$, the space function $\mathbf{G} \in R^{2n} \times R^n \times R^m$. One from the solutions of Eq. (6) has the form Eq. (8). This solution corresponds to the moment of motion perturbation.

2.1 Stability in the sense of Lyapunov

The problem of stability in the Lyapunov sense [18-30] of the gripping device motion is formulated as an analysis of stability of the equations of the perturbed motion, as a function of $\varepsilon, \mathbf{\Delta}$

$$\mathbf{y} = 0\,. \tag{8}$$

Lyapunov exponents associated with a trajectory are a measure of the average rates of expansion and contraction of the trajectories surrounding it. They are asymptotic quantities, defined locally in the state space, and describe the exponential rate, at which a perturbation to a trajectory of a system grows or decays with time at a certain location in the state space. The Lyapunov exponents calculated for the nonlinear system are described by [19-34]

$$\lambda_i = \lim_{t\to\infty} \frac{1}{t} \ln |m_i(t)|\,, \qquad i = 1, ..., 2n\,, \tag{9}$$

where all of the m_i are the eigenvalues of matrix of the fundamental solutions of linearized equation of perturbation. The procedure used to determine the Lyapunov exponents can be considered as a generalization of linear stability analysis. The Lyapunov exponents are global quantities associated with an attractor even though they are defined only locally in the state space. From this point of view the method of analysis of behaviour of the system will be called nonlinear.

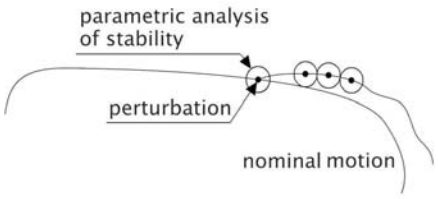

Figure 1: Discrete parametric analysis of the system behaviour in the close neighborhood of the perturbed motion.

2.2 Linear analysis of stability in close neighborhood of the moment of perturbation

In Fig. 1 an idea of the stability analysis in the neighborhood of the perturbed motion is presented.

It is possible to control the system by analysis of eigenvalues calculated in a close neighborhood of the trajectory. As a result of linearization of the Eq. (6) in the vicinity of the perturbation point $\mathbf{q}(t)$, the Eq. (7) has the form

$$\dot{\mathbf{y}} = \mathbf{A}^* \mathbf{y}\,, \tag{10}$$

where $\mathbf{A}^*(\mathbf{q}, \dot{\mathbf{q}}, \ddot{\mathbf{q}}, \varepsilon, \boldsymbol{\Delta})$ is the Jacobian matrix. As can be seen, the coordinates of the matrix $\mathbf{A}^*$ depend on the control system parameters, Eq. (5), on the manipulator's main parameters, Eq. (14), and on the generalized coordinates of the nominal motion of the manipulator's links.

Analysis of stability of the column matrix (8) is reduced then to the analysis of its eigenvalues. In order to perform this analysis, we have to generate the matrix $\mathbf{A}(t)$ composed of the derivatives of the equations of perturbed motion, Eq. (6), as a function of parameters of perturbations, Eq. (4), in the form

$$\mathbf{A}(t) = \frac{\partial f_i(\mathbf{y}_{i0})}{\partial \mathbf{y}_i} \tag{11}$$

for the set of conditions $\mathbf{y}_0$ for the given time instant and where Eq. (6) is $\dot{y} = f(y, t)$. The eigenvalues of the perturbation equations in the vicinity of the perturbation conditions can be determined from the determinant

$$\det[\mathbf{A}(t) - \boldsymbol{\Lambda}\mathbf{I}] = 0\,, \tag{12}$$

where $\mathbf{A}(t) \in R^{2n\times 2n}$ is the Jacobi matrix in the point $\mathbf{y}_0$, $\overline{\Lambda}$ – the vector of eigenvalues, and $\mathbf{I}$ – the unit matrix, $\mathbf{I} \in R^{2n\times 2n}$.

The roots of Eq. (12) determine regions of stability. The solution in the close neighborhood of the perturbation has tendency to be stable, if eigenvalues are negative or equal to zero. Analysis of the eigenvalues in the vicinity of perturbation point allows to determine the behaviour of the system in close neighborhood of perturbation. This behaviour shows tendency of the system to be / not to be stable. As a result we can determine parametric regions of stability. Analysis of the eigenvalues in vicinity of the perturbation point is linear analysis of stability.

2.3 Poincaré maps

Algorithms for the numerical continuation of the periodic solutions are quite sophisticated [2-22]. These algorithms have been extensively used for computing the forced response and limit cycles of the nonlinear dynamical systems.

The Poincaré maps in the paper were used as an additional tool for graphical presentation of stability areas of the nonlinear system. In the vicinity of the Eq. (8), the Poincaré map has been expressed as a set

$$\{[\psi_i(t), \dot{\psi}_i(t)]\,|_{t=t_0+k\cdot T}\,, i = 1, ..., n, k = 1, 2, ...\}\,, \tag{13}$$

where t_0 is the moment of the motion perturbation, T – the period of the gripping device motion along the trajectory of its motion.

As can be seen in Eq. (13), the procedure can not be used to control in the real-time motion.

2.4 Parametric analysis of stability

The stability analysis has been conducted in order to determine the stability regions. It has also consisted identification of influence of the manipulator's model parameters to a type of its behavior. These parameters can be divided into three groups. The first one concentrates on the kinematics of the gripping device, the second one is related to its motion trajectory, and the third one is discusses the stiffnesses and damping in the driving systems and rolling of the kinematics pairs. A set of the parameters that can to be investigated is

$$\varepsilon = \begin{bmatrix} \text{kinematics of gripping device} \\ \text{trajectory parameters} \\ \text{stiffness and damping} \end{bmatrix}, \tag{14}$$

where $\varepsilon \in R^m$. Some exemplary parameters of these groups have been presented in Sections 4.2 and 4.3. A selection of values of the set of parameters ε results in a defined type of the manipulator's behavior. Such a procedure allows finding a relationship between the set ε, defined by Eq. (14), and the type of manipulator's behavior, that is to say, the character of its oscillations.

3 Maps of stability subregions, stability control

Bifurcation maps of stability regions, performed on the basis of Eqs. (9),(13), are called maps of nonlinear stability of dynamical system. These maps have been made in function of a set of parameters of the Eq. (14). On the other hand, if we assume a close neighborhood of the matrix (8), then the linear analysis of stability in the vicinity of Eq. (8) using analysis of eigenvalues can be assumed as an approximation. This approximation affects manipulator's stability regions in an unknown way. Although the linearization helps determining whether a perturbation point is stable or not, it does not provide any information regarding the size of the domain around the perturbation point, where the conditions of stability holds. Therefore, in order to analyze the manipulator's stability

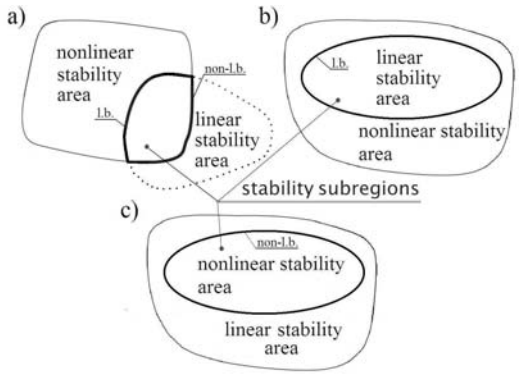

Figure 2: Ways of stability subregions analysis using map of the Lyapunov exponents for the assumed range of the motion perturbations. Description: (l.-b.) denotes the linear boundary of stability and (non-l.b.) the nonlinear one.

subregions, the analysis of stability regions for the nonlinear system using the linearized equations of perturbation has been suggested.

Generally, the ranges of parametric stability of the nonlinear and linear system do not correspond in the vicinity of the perturbation point. Therefore, it is proposed to separate the common parts of these regions (stability subregions). We can distinguish the following cases of the stability position of the nonlinear and linear system, (Fig. 2(a–c)):

(i) linear and nonlinear regions have a common part, Fig. 2a)

(ii) linear range inside the nonlinear range, Fig. 2b)

(iii) nonlinear range inside the linear range, Fig. 2c)

(iv) linear and nonlinear ranges without a common part: This situation is possible, if the correcting control signal appears in the control system in spite of absence of the motion perturbation, or, if the maps of the linear stability have been built for oversized ranges of the motion perturbations.

Maps of the linear stability have been constructed for certain ranges of the perturbations of the manipulator's state vector. Assumed ranges of the perturbations have decided about the size and position of the linear stability regions and about number of stability maps in the control system memory. As a result we have received the so-called stability subregions from the common part of the stability regions of the nonlinear system (by use of the Lyapunov exponents) and the linearized equations of perturbation in close neighborhood of the perturbation point (the vector of eigenvalues), Figs. 2(a–c).

Such a procedure allows avoiding of the effect of errors resulting from any simplification assumed in the mathematical model of the manipulator, and, first of all, for generation of the maps of the stability subregions as a function of ranges, in which the motion perturbations can occur. For a given map, the size of the stability subregions is related of course to the assumed perturbation ranges. In practice, in order to achieve the control of motion, it is easy to calculate the vector of eigenvalues and determine the values of the control parameters from the map of the stability subregions by simple measurement of the real perturbations. Of course, the set of such maps of the subregions stability should stay in the memory of the system control unit.

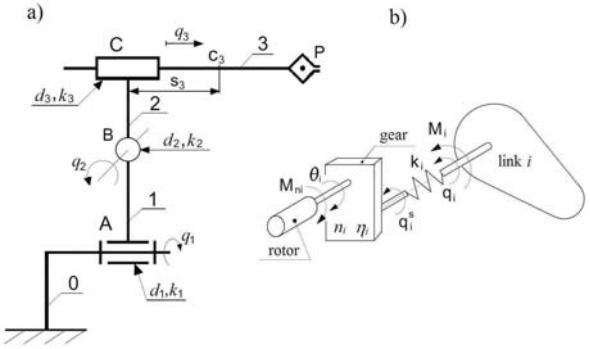

Figure 3: a) Kinematics scheme of the manipulator. b) Model of the driving systems, where n_i denotes the gear ratio, η_i the mechanical efficiency of the gear.

4 Model of the manipulator 7MAR

The 7MAR industrial manipulator, Fig. 3a, whose main data can be found in [36-], has been the subject to the numerical analysis. In order to determine the stability regions of the nonlinear and linearized systems, it is necessary to build the mathematical model of the manipulator and its drive systems. The model is important in the identification of nonlinear areas of the stability [19-36]. In the proposed method, the stability subregions that allow simplifications in the mathematical model have been separated from the common part of the stability regions of the nonlinear and the linearized systems. Generally speaking, the smaller the stability subregion in the stability zone, the more simplifications in the mathematical model, or, generation of a single map of stability regions for a higher range of motion perturbations are possible. The electric and mechanical model of the driving system of the manipulator covers the torsional flexibilities, viscous damping and resistance to friction in the driving systems. In Fig. 3b, the model of the driving systems is presented. It has been assumed that each link is driven by an independent driving system and consists of an electric motor, a mechanical gear and driving shafts. A stator of the driving motor of the i-th driving system is connected with the $(i-1)$-th link. Energy losses due to mechanical clearances in driving units and the gyroscopic effects between motors and manipulator links have been neglected.

The kinetic energy of the manipulator is defined by

$$E_k = \frac{1}{2}\left[\dot{\mathbf{q}}^T\mathbf{D}(\mathbf{q})\dot{\mathbf{q}} + (\dot{\mathbf{q}}^s)^T\mathbf{I}_{zr}\dot{\mathbf{q}}^s\right] , \tag{15}$$

where $\mathbf{D}(\mathbf{q})$ is matrix of inertia of the manipulator links, $\mathbf{I_{zr}}$ represents matrix of moments of inertia of rotors of the driving motors, power transfer shafts and rotating elements of the reductions gears reduced to the corresponding generalized coordinates of the links, $\mathbf{q}$ is vector of generalized coordinates of links, and, $\mathbf{q^s}$ is the vector of generalized coordinates of driving systems.

The potential energy of the manipulator has been expressed as a sum of the potential energy of links, an object being manipulated, elements of power transfer systems and flexibility in the driving systems. The potential energy of flexibility of driving systems is

described by a matrix of resultant torsional stiffnesses of the power transfer systems. The potential energy of the elements of the power transfer systems is equal to

$$E_p^d = \sum_{i=1}^{n}\sum_{j=1}^{l} E_{pij}^n = \sum_{i=1}^{n}\sum_{j=1}^{l_1} E_{pij}^n + \sum_{i=1}^{n}\sum_{j=l_1+l}^{l=l_1+l_2} E_{pij}^n \,, \tag{16}$$

where E_{pij}^n is the potential energy of the j-th element of the i-th manipulator driving system; l_1,l_2 are numbers of elements of the driving system of the link i assigned to the link $(i-1)$ and i, respectively.

The viscous friction in the driving system is a sum of the viscous friction in the driving motor and the viscous friction in the remaining part of the driving system reduced to the axis of the driving motor. Generally, for all the driving systems we have equations of motion in the form

$$\mathbf{I}_{zr}^* \ddot{\theta} + \mathbf{N}^{-1}\mathbf{K}(\mathbf{N}^{-1}\theta - \mathbf{q}) + \mathbf{B}\dot{\theta} = \mathbf{Q}_d \,, \tag{17}$$

where $\mathbf{N}$ is diagonal matrix of reduction gear ratios of driving systems; $I_{zr}^* = I_{zr}/N^2$ is the diagonal matrix of inertia of driving systems reduced to the corresponding axis of the driving motors; $\ddot{\theta}$ is vector of angular positions of rotors; $\mathbf{Q_d}$ describes the vector of the driving quantities of the links reduced to the axis of driving motors; $\mathbf{K}$ is the diagonal matrix of stiffnesses in the driving systems reduced to the corresponding generalized coordinates of the links; $\mathbf{B}$ represents diagonal matrix of viscous damping in the driving systems (notation d in Fig. 3) that has been expressed as follows

$$\mathbf{B} = \mathrm{diag}\left[f_{w1} + \sum_{l=1}^{w^1} f_{u1}^l,\ f_{wi} + \sum_{l=1}^{w^i}, f_{ui}^l, \ldots, f_{wn} + \sum_{l=1}^{w^n} f_{un}^l \right] , \tag{18}$$

where w^i states the number of elements of the i-th driving system that are considered in determination of viscous friction; f_{wi} is coefficient of viscous damping in the i-th driving motor; $\sum_{l=1}^{w^i} f_{w,un}^l$ represents sum of coefficients of viscous damping of individual elements of the power transfer system reduced to the axis of the i-th driving motor. Generally, the equations of motion of the manipulator assume the form

$$\mathbf{M}\ddot{\mathbf{q}}_m + \mathbf{C}(\mathbf{q}_m, \dot{\mathbf{q}}_m) + \mathbf{K}_g\mathbf{q}_m + \mathbf{G} = \mathbf{Q} \,, \tag{19}$$

where $\mathbf{M}$ is matrix of masses and inertia of the manipulator, $\mathbf{C}$ matrix of effects of gyroscopic forces, centrifugal forces and energy dissipation. $\mathbf{K}_g$ is matrix of the manipulator stiffnesses. The procedure of calculating the coefficients of stiffnesses can be found in [37]; $\mathbf{G}$ describes matrix of gravity forces; $\mathbf{Q}$ vector of the driving quantities; $\mathbf{q}_m = [\mathbf{q}, \theta]^T$ is the vector of generalized coordinates of the manipulator.

The manipulator performs its technological task in two steps. The first one means a motion in the first driving system and the second one a motion of the second and third degree of freedom, whereas the first degree is stationary. During the second step of motion, after introducing perturbations into second and third generalized coordinates Eq. (3) it has form

$$q_p = q_p + \psi_p \,, \quad \dot{q}_p = \dot{q}_p + \dot{\psi}_p \,, \tag{20}$$

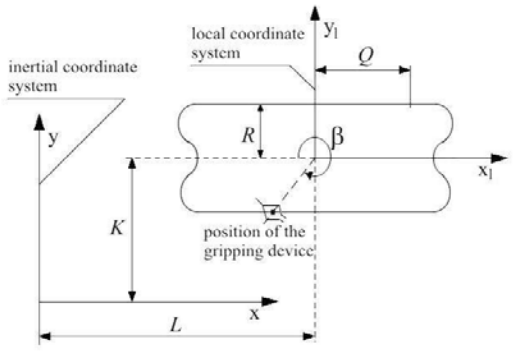

Figure 4: Parameters of the trajectory of the gripping device motion.

where $p = 1, 2$, we obtain nonlinear first order differential equations of the perturbations

$$\dot{\mathbf{y}} = a_{\mathbf{l}}\mathbf{y} + \mathbf{b_l}\boldsymbol{\Delta}_{\mathbf{n}} + \mathbf{c}^{\mathbf{2}}_{\mathbf{n}}(\mathbf{y}) + \mathbf{d}^{\mathbf{2}}_{\mathbf{n}}(\mathbf{y}, \dot{\mathbf{y}}) + \mathbf{c}^{\mathbf{3}}_{\mathbf{n}}(\mathbf{y}) + \mathbf{d}^{\mathbf{3}}_{\mathbf{n}}(\mathbf{y}, \dot{\mathbf{y}}) \tag{21}$$

where: $\mathbf{a}_l$, $\mathbf{b}_l$ are matrices of the linear parts of the equations of motion, $\mathbf{c}^2_n(\mathbf{y})$, $\mathbf{d}^2_n(\mathbf{y}, \dot{\mathbf{y}})$, $\mathbf{c}^3_n(\mathbf{y})$, $\mathbf{d}^3_n(\mathbf{y}, \dot{\mathbf{y}})$ are matrices of second and third order of the nonlinearity (depending on $\mathbf{y}$ and $\dot{\mathbf{y}}$), and, $\boldsymbol{\Delta}_n$ is the vector of compensating drive in the second and third driving system.

4.1 Trajectory and kinematics of the manipulator

The trajectory of the manipulator gripping device motion is presented in Fig. 4. We assumed periodic trajectory of motion as a typical trajectory of industrial machines. The position of the gripping device on its trajectory is described by an angle β in the local coordinate system $X_l Y_l 0_l$, see Fig. 4. It is possible to analyze the manipulator nominal motion as a function of an angle β.

4.2 Analysis of stability, bifurcations and strange chaotic attractors

The Lyapunov exponents are calculated for varying parameters of the velocity of the gripping device motion along the motion trajectory and for control parameters, Eq. (14). In the manipulator under consideration, the linear control has been applied. The model of the control system has the form

$$\Delta M_2 = aU_s\,, \quad \Delta M_3 = bU_s\,, \tag{22}$$

where ΔM_i, $i = 2, 3$ are the compensating driving quantities, U_s is the controlled variable (common for the second and third driving systems). The coefficient a is connected with the second drive system, whereas the coefficient b with the third drive system. The simplest algorithm of control allows showing, in an easy way, the spectrum of bifurcations which can be found also for more complex control systems [19]. The analysis has been

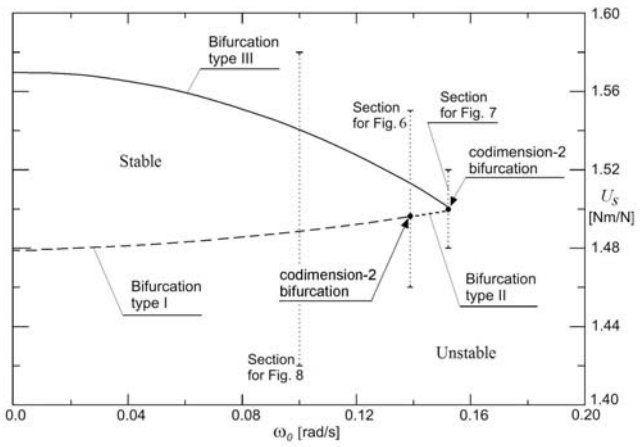

Figure 5: Stability as a function of control parameter U_s and the kinematics of the gripping device.

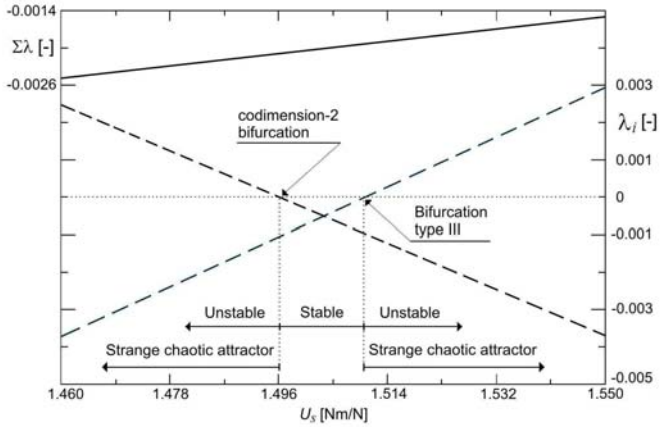

Figure 6: Spectrum of the Lyapunov exponents for the data presented in Figure 5 and $\omega = 0.1406$ rad/s.

conducted for the perturbations of positions and motion velocities of the second and third link. Below, a few sample diagrams of stability regions for the angle of the gripping device position $\beta = 5.5$ rad (perturbations occur at the instant when the gripping device is in this position, Fig. 4), are shown. The data concerning the motion trajectory of the gripping device are: $K = 0.5$ m, $L = 0.231$ m, $R = 0.05$ m, $Q = 0.05$ m. At the figures that show the spectra of the Lyapunov exponents, the broken lines represent two Lyapunov exponents.

In Fig. 5, a boundary of stability as a function of the control coefficient U_s and the angular velocity of the gripping device motion for the coefficients $a = -45.6$, $b = -0.003$ is depicted. The ranges of parameters for which the system is stable and the types of bifurcations which can occur during a loss of stability are seen. A selection of control parameters from the stability region allows for maintaining the motion stability in the Lyapunov sense. Each bifurcation allows one to identify vibrations that occur

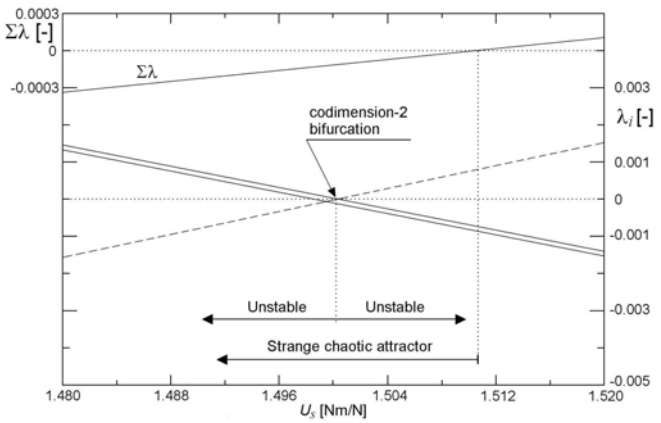

Figure 7: Spectrum of the Lyapunov exponents for the data presented in Figure 5 and $\omega = 0.1519$ rad/s.

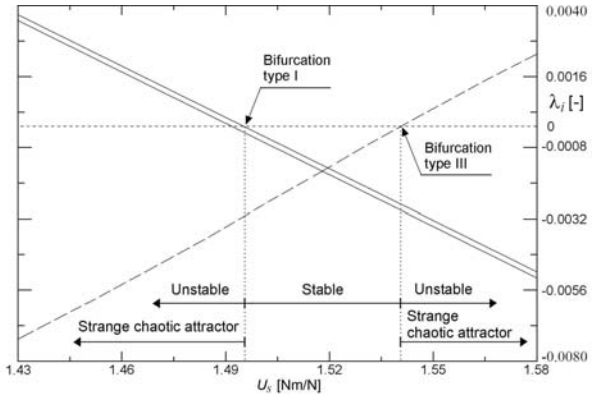

Figure 8: Spectrum of the Lyapunov exponents for the data presented in Figure 5 and $\omega_0 = 0.1$ rad/s.

after the stability loss of motion. Type I bifurcation is a saddle-node bifurcation. Type II bifurcation is a double-period bifurcation. In this case, the stable periodic trajectory with the period T is replaced by the trajectory with the period $2T$. Type III bifurcation is a secondary Hopf bifurcation [3-19-25]. In this case, the periodic solution transforms into a quasi-periodic one and, therefore, this type of bifurcation is the least disadvantageous from the point of view of the motion control.

Apart from this, it is seen in Fig. 5 that in the case of manipulators, bifurcations with codimension 2 can be found. In the first case of a codimension 2 bifurcation, the stability loss occurs due to the simultaneous occurrence of a saddle-node bifurcation and a double-period bifurcation. As can be seen in Fig. 6, in the bifurcation point, a decomposition of the 2-dimensional unstable torus that represents the quasi-periodic motion occurs. The torus decomposes and the motion along it is replaced by a motion on a strange chaotic attractor. In the second case, the stability loss is due to the simultaneous occurrence of a double-period bifurcation and a secondary Hopf bifurcation.

The stability loss takes place through a decomposition of the 3-dimensional unstable

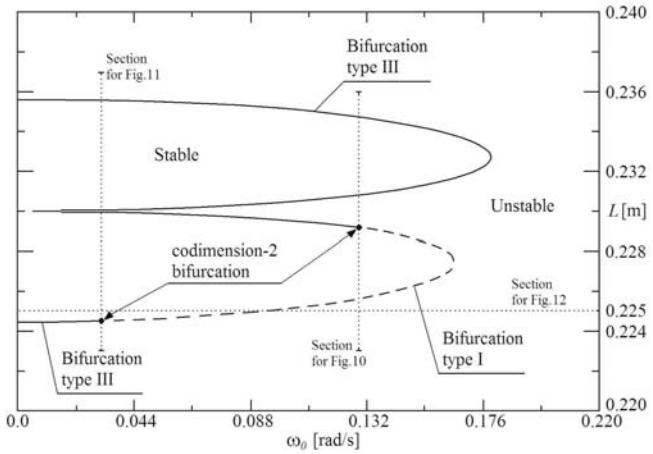

Figure 9: Stability loss as a function of the dimension L, Figure 4, and the kinematics of the gripping device motion.

torus, Fig. 7, that represents the quasi-periodic motion with three frequencies, between which there are no rational relationships. This mechanism leads to motions on strange chaotic attractors. As shown in Fig. 7, after the manipulator stability loss, a motion on the strange chaotic attractor occurs, but only for a certain variable of the driving system control. Above the value $U_s = 1.5108$ Nm/N, the system does not have an attractor, and the system shows a tendency towards the escape to infinity. An influence of the driving system control variable U_s on the stability and the character of motion after its stability loss is visible. In Fig. 8, a spectrum of Lyapunov exponents for the data from Fig. 5 and $\omega_0 = 0.1$ rad/s is presented.

The stability loss occurs through a saddle-node bifurcation and a secondary Hopf bifurcation. As a result of these bifurcations, unstable tori appear. As a result of their decompositions, the quasi-periodic motion is replaced by a motion on the strange chaotic attractor. This attractor is present in the whole unstable range of the system. In this case, the system has an attractor and because of this the loss of stability is not so disadvantageous. In Fig. 9, we can see a stability region and types of bifurcations as a function of the quantity L of the position of the motion trajectory, Fig. 4, and the velocity of motion of the gripping device along the trajectory of its motion. The following values of the control coefficients have been assumed: $U_s = 1.51$ Nm/N, $a = -45.6$, $b = -0.003$. An influence of the position of the trajectory of motion of the gripping device on the manipulator stability region and bifurcation type is visible. During the stability loss, it is possible that all three types of bifurcation with codimension 1 and a bifurcation with codimension 2 for $\omega_0 = 0.0316$ rad/s and 0.129 rad/s will occur. The bifurcation with codimension 2 is in this case a combination of a secondary Hopf bifurcation and a saddle-node bifurcation. The stability loss occurs through the occurrence and simultaneous decomposition of the unstable 3-dimensional torus. The spectrum of Lyapunov exponents for $\omega_0 = 0.129$ rad/s is shown in Fig. 10. As can be seen, such ranges are possible to occur when the system has a strange chaotic attractor, which however ceases quickly to exist. In practice, after the stability loss, the system does not have an attractor. A similar situation concerns

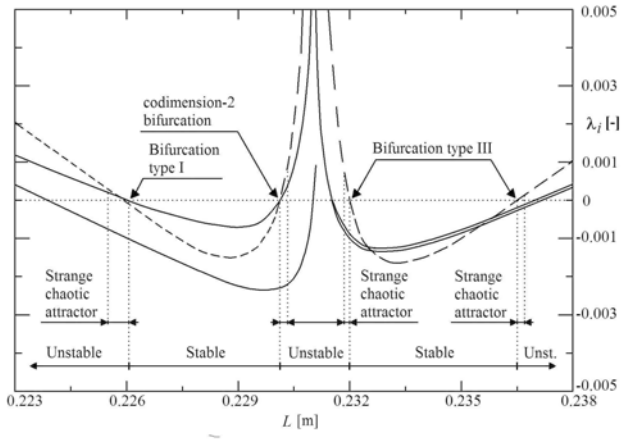

Figure 10: Spectrum of the Lyapunov exponents for the data presented in Figure 9 and $\omega_0 = 0.129$ rad/s.

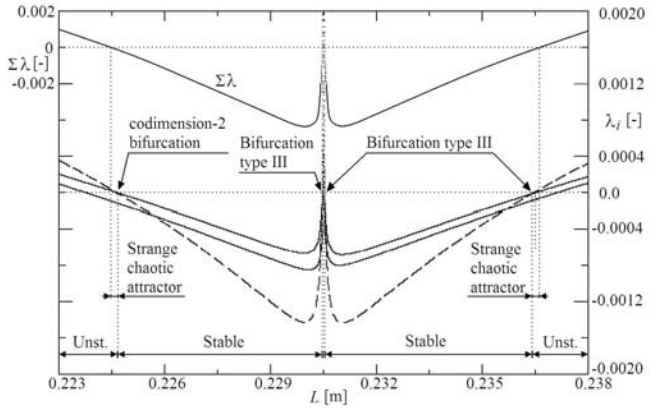

Figure 11: Spectrum of the Lyapunov exponents for the data presented in Figure 9 and $\omega_0 = 0.0316$ rad/s.

the second bifurcation point with codimension 2 ($\omega_0 = 0.0316$ rad/s), whose vicinity is shown in Fig. 11 in the form of the spectrum of Lyapunov exponents. The regions of stability and the ways of the stability loss are visible. Fig. 12, an influence of the angular velocity of the gripping device motion along the periodic trajectory on the stability regions and the ranges of occurrence of a strange chaotic attractor can be seen. Thus, both the control coefficients and the control variable, as well as the kinematics of the gripping device motion exert an influence on the way of the stability loss and the type of vibrations that occur after it. Vibrations that occur in the system accompany each kind of bifurcation. During the stability loss, a bifurcation with codimension 2 can occur. It is interesting to find this kind of bifurcation for such a system. For the defined sets of model parameters, two bifurcations occur at the same time. We tend to eliminate a possibility of such phenomena through maintaining the operation of driving systems within ranges of a stable motion.

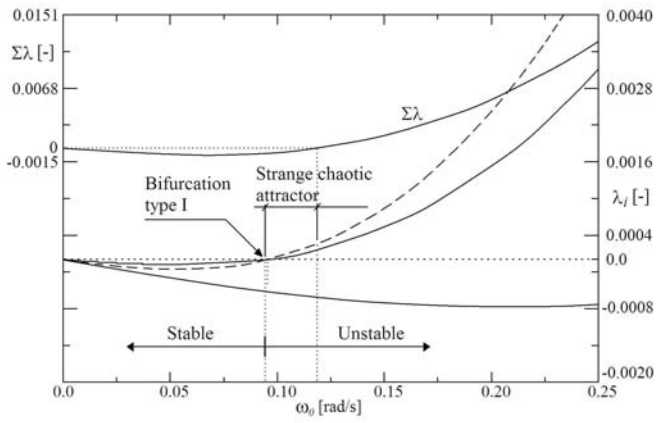

Figure 12: Spectrum of Lyapunov exponents for the data presented in Figure 9 and $L = 0.225$ m.

4.3 Maps of stability and control

In Fig. 13, a spectrum of the Lyapunov exponents as a map is proposed. This kind of map is introduced for choosing the values of control parameters for which the manipulator remains stable. The presented regions of stability are the resultant regions of stability obtained on the basis of the analysis of the nonlinear system (Poincaré maps, Eq. (13) and Lyapunov exponents Eq. (9)) and by means of the linearized equations of perturbation, Eq. (12). Besides, a way of transition from stability to a strange chaotic attractor as a function of the angular velocity of the gripping device motion and the control variable is presented. As can be seen, for a certain value of the angular velocity ω_0 that depends on the U_s, only a region without a manipulator attractor occurs. Below this velocity, a loss of stability leads to chaotic vibrations, regardless of the bifurcation type that causes this stability loss. Thus, there is a certain boundary value of the velocity ω_0 below which the system has an attractor and in which region of the control system should maintain the manipulator. A selection of values of the control parameters a, b from the range of a strange chaotic attractor gives rise to chaotic vibrations of the manipulator. As can be seen from the above-mentioned figures, the spectrum of Lyapunov exponents and the proposed maps of Lyapunov exponents are useful for control. Measures of perturbations which can occur during motion can be quickly presented in the form of the spectrum of their eigenvalues (the Lyapunov exponents). Next, from the maps of the stability subregions, it is easy to find for which values of control parameters the manipulator remains stable. On the other hand, Fig. 14 shows stability regions and types of induced vibrations as a function of the coefficients a and b for the control parameter $U_s = 1.51$ Nm/N and the angular velocity equal to 0.1 rad/s. In Fig. 14 two kinds of bifurcation with codimension 1 are possible: a saddle-node bifurcation and a secondary Hopf bifurcation. Apart from this, a bifurcation with codimension 2 is possible as well. Such a bifurcation with codimension 2 is composed of a secondary Hopf bifurcation and a saddle-node bifurcation.

The stability loss in the Lyapunov sense, resulting from the occurrence of this bifurcation, consists in the appearance and decomposition of a 3-dimensional torus. The quasi-periodic solution is unstable. Fig. 15 presents a map of Lyapunov exponents which

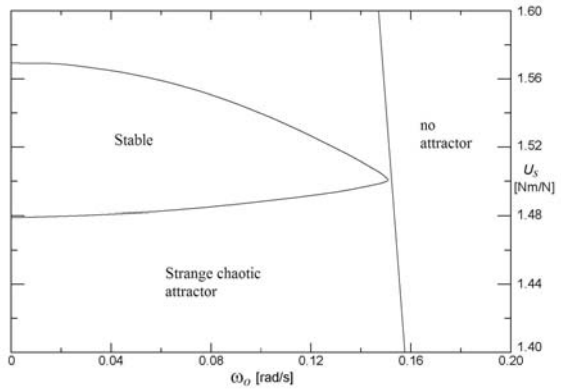

Figure 13: Map of stability and regions of strange chaotic attractors as a function of control parameter U_s and kinematics of gripping device.

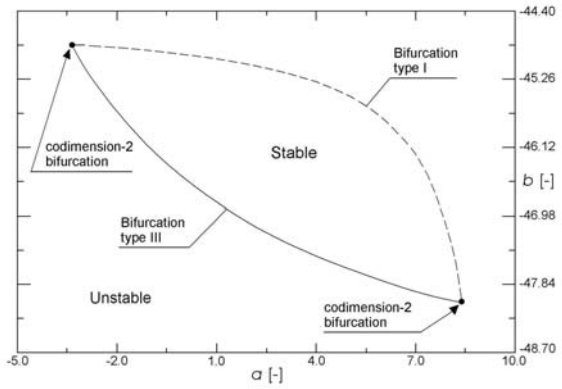

Figure 14: Stability losing as a function of control coefficients a and b.

shows a stable region and regions with a strange chaotic attractor or without it.

The ways of transition between the stable region and the remaining regions are interesting. A loss of stability by a bifurcation with codimension 2 is possible, Fig. 14, then vibrations occur on a strange chaotic attractor or the system escapes to infinity when the manipulator does not have an attractor. A loss of stability by a bifurcation with a codimension 1 leads to vibrations on a strange chaotic attractor.

In Fig. 16 a map which shows a way in which a stability loss leading to vibrations on a strange chaotic attractor occurs, regardless of the bifurcation co-dimension and its type, is shown. Narrow ranges of the values of control coefficients corresponding to the region of a strange chaotic attractor cause that the system escapes easily to the region where there is no attractor. In Fig. 17 a map of the regions of attractors for the gripping device position angle $\beta = 0.96$ rad is shown. In this case, we have only the regions with a strange chaotic attractor or the regions without an attractor. There is no stable region. A perturbation of the manipulator motion for the ranges of control coefficients shown leads to one of these regions and is particularly disadvantageous from the viewpoint of motion control.

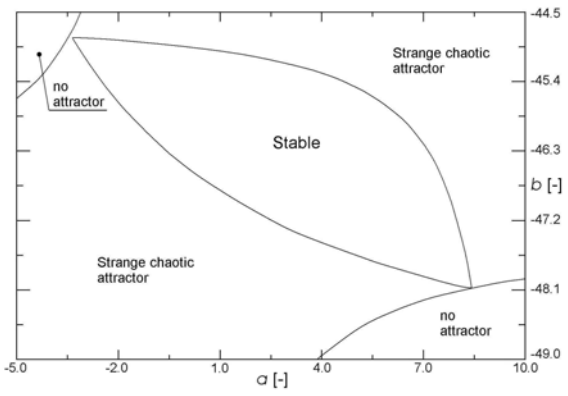

Figure 15: Map of stability and regions of strange chaotic attractors as a function of control coefficients a and b.

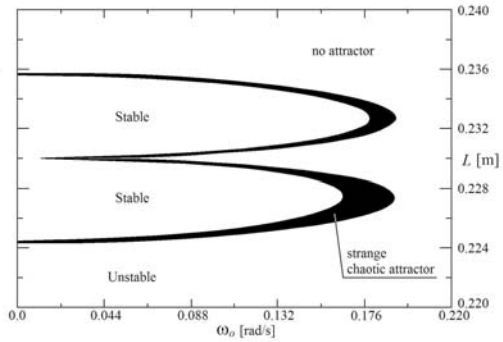

Figure 16: Map of stability and strange chaotic attractors regions as a function of the dimension L, Figure 4, and the kinematics of the gripping device.

Vibrations that occur in the system accompany each kind of bifurcation. During the stability loss of the model, a bifurcation with codimension 2 can occur. Finding this kind of bifurcation for such system is interesting. For the defined sets of model parameters, two bifurcations occur at the same time. The stability loss occurs through the decompositions of unstable, multidimensional tori that represent quasi-periodic vibrations. As a result, we obtain a strange chaotic attractor or a lack of the attractor, that is to say, a tendency of the system to the escape to infinity. We tend to eliminate a possibility of such phenomena occurrence through maintaining the operation of driving systems within ranges of a stable motion. A proper selection of values of control coefficients that depend on a perturbation allows for avoiding regions with a strange chaotic attractor or without it. In Fig. 18, an algorithm for the manipulator motion control has been proposed. This kind of control was qualified to nonlinear methods. The library in the control memory includes a set of stability maps drawn as a function of selected model parameters and as a function of perturbation ranges of individual degrees of freedom. The range of the coefficients a, b and the driving system control variable U_s and the positions of the trajectory, as well as the kinematics of the gripping device motion exert an influence not only on the motion stability but also on the character of motion after the stability loss. The stability loss of

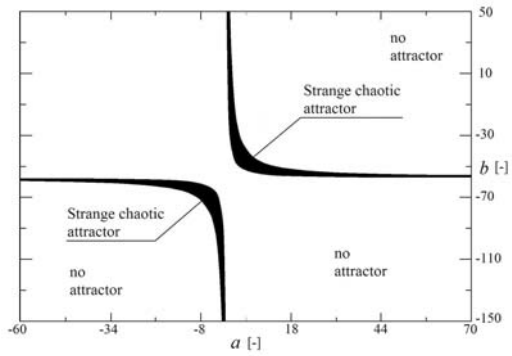

Figure 17: Regions of the strange chaotic attractors for the angle of the gripping device position $\beta = 0.96$ rad (Figure 4).

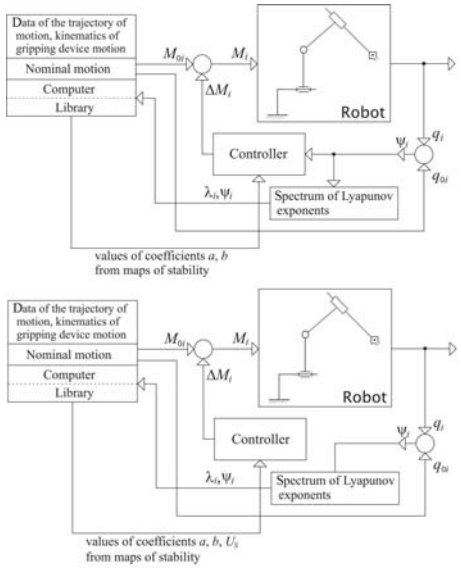

Figure 18: Schemes of the control systems.

the system should be avoided, however if it occurs, we should aim at the situation where the system has an attractor, even a chaotic one. It allows us to control the system during the stability loss. An idea of controllers used in the control systems is presented in Fig. 19. The controller defines a value of the moment ΔM, Eq. (22), on the basis of the coefficients a, b which are read from the correspond stability map. The control variable U_s is defined on the basis of measured perturbation ψ and some mathematical formula – Fig. 19a) or from map of stability which correspond to the value of perturbation – Fig. 19b).

As can be seen from the figures included in the paper, the analysis of the spectrum of Lyapunov exponents is a quick and simple method to parametric identify the stability regions in the Lyapunov sense, the threat of a loss of stability, the way the stability loss occurs and the kind of induced vibrations. From this point of view, it can be a valuable tool to control the motion. The proposed maps of Lyapunov exponents allow one to find

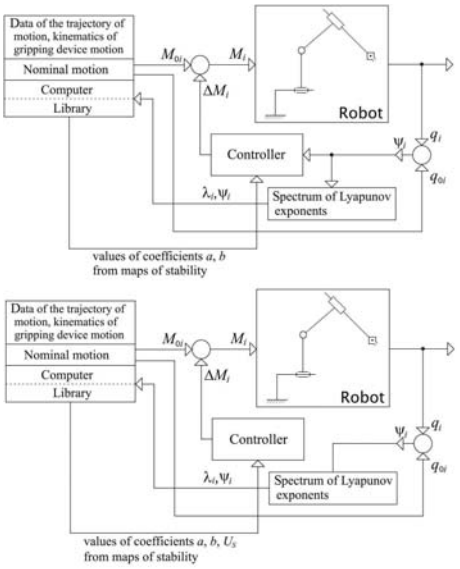

Figure 19: The controller loop with U_{si} linear depending on Ψ_i – a), and U_{si} taking from the map of stability - b).

values of control parameters for given motion perturbations. The main advantages of the proposed control rest on possibility of using this algorithm in real time despite of nonlinear analysis of the system.

5 Conclusions

In the paper a method of control of the manipulator motion from the nonlinear dynamics point of view is presented. The spectrum of Lyapunov exponents in the map form has been proposed as a tool to control motion. The control of motion is based on the analysis of stability regions of the nonlinear system and linearized equations of perturbation and on the generation of the so-called maps of stability. These maps are used in order to determine the values of control parameters, for which the manipulator remains stable after introducing perturbations to its motion. The method permits to control the nominal motion, to investigate the tendency towards a stability loss and to select a return way to the stability region by avoiding the chaotic vibration induction.

A method allows also for the parametric analysis of mode of vibrations. The algorithm allows for a theoretical analysis of an influence of manipulator model parameters on the ways the manipulator stability is lost and on the regions in which a strange chaotic attractor occurs or does not occur. A possibility of ways the strange chaotic attractor appear have been presented as well.

Acknowledgement

This paper is the last work of Dr. Przemyslaw Szumiński who died on 24 October 2011 at the age of 44.

References

[1] Abed, E.H. and Fu, H.-J., "Local feedback stabilization and bifurcation control. II. stationary bifurcation", *Systems Control Letters*, 8, 467-473, 1987.

[2] Abed, E.H., Wang, H.O., Chen, R.C., "Stabilization of period doubling bifurcations and implications for control of chaos", *Physica D*, 70, 154-164, 1994.

[3] Bishop, S.R. and Kapitaniak, T., The Illustrated Dictionary of Nonlinear Dynamics and Chaos, *J.Wiley & Sons*, London, 1999.

[4] Braiman, Y. and Goldhirsch, I., "Taming chaotic dynamics with weak periodic perturbations", *Physics Review Letters*, 66, 2545-2548, 1991.

[5] Caracciolo, R., Gasparetto, A., Giovagnoni, M., Trevisani, A., "On the control of flexible link manipulators: results of two numerical investigations", *Proceedings of the 12th International Workshop on Robotics in Alpe-Adria-Danube Region (RAAD'03)*, Cassino, Italy, 2003.

[6] Chen, S., Zhang, Q., Xie, J., Wang, C., "A stable-manifold-based method for chaos control and synchronization", *Chaos, Solitons and Fractals*, 20, 947-954, 2004.

[7] Ditto, W.L., Rauseo, S.N., Spano, M.L., "Experimental control of chaos", *Physics Review Letters*, 65, 3211-3214, 1990.

[8] Doedel, E.J., Keller, H.B., Kernevez, J.P., "Numerical analysis and control of bifurcation problems (I) Bifurcation in finite dimensions", *International Journal of Bifurcation and Chaos*, 1, 493-520, 1991.

[9] Dombre, E. and Khalil, W., Robot Manipulators. Modeling, Performance Analysis and Control, *Wiley–Blackwell*, 2007.

[10] Dressler, U. and Nitsche, G., "Controlling chaos using time delay coordinates", *Physics Review Letters*, 68, 1-4, 1992.

[11] Fuller, C.R., Elliott, S.J., Nelson, P.A., Active control of vibration, *Academic Press Limited*, London, 1996.

[12] Gawronski, W., Ih, C.H., Wang, S.J., "On dynamics and control of multi-link flexible manipulators", *Journal of dynamic Systems, Measurement, and Control*, 117, 134-142, 1995.

[13] Ge, Z.-M., Chang, C.-M., Chen, Y.-S., "Anti-control of chaos of single time scale brushless dc motors and chaos synchronization of different order systems", *Chaos, Solitons and Fractals*, 27, 1298-1315, 2006.

[14] Glendinning, P., Stability, Instability and Chaos, *Cambridge University Press*, 1995.

[15] Gonzalez-Miranda, J.M., Synchronization and control of chaos, *Imperial College Press*, London, 2004.

[16] Iooss, G. and Joseph, D.D., Elementary Stability and Bifurcation Theory, *Springer*, New York, 1981.

[17] Kapitaniak, T., Chaotic oscillations in mechanical systems, *World Science*, Manchester University Press, 1991.

[18] Kapitaniak, T., Controlling chaos, *Academic Press*, London, 1996.

[19] Kapitaniak, T., Chaos for engineers: theory, applications and control, *Springer-Verlag*, Heidelberg, 2000.

[20] Li, C. J. and Sankar, T. S., "Systematic methods for efficient modeling and dynamics computation of flexible robot manipulators", *IEEE Transactions of System Man and Cybernetics*, SMC-23(1), 77-94, 2006.

[21] Magnitskii, N. A. and Sidorov, S. V., "New methods for chaotic dynamics", *Scientific Series on Nonlinear Science A*, **58**, 2006.

[22] Manffra, E. F., Caldas, I. L., Viana, R.L., "Stabilizing periodic orbits in a chaotic semiconductor laser", *Chaos, Solitons and Fractals*, 15, 327-341, 2003.

[23] Morel, C., Bourcerie, M., Chapeau-Blondeau, F., "Generating independent chaotic attractors by chaos anticontrol in nonlinear circuits", *Chaos, Solitons and Fractals*, 26, 541-549, 2005.

[24] Nahvi, N. and Ahmadi, H., "Dynamic Simulation and Nonlinear Vibrations of Flexible Robot Arms", *Journal of Applied Sciences*, 3(7), 510-523, 2003.

[25] Nayfeh, A. H. and Balachandran, B., Applied nonlinear dynamics – Analytical, Computational, and Experimental Methods, *Wiley-VCH*, 2004.

[26] Ott, E., Grebogi, C., Yorke, J. A., "Controlling chaos", *Physics Letters Review*, 64, 1196-1199, 1990.

[27] Peeters, M., Viguie, R., Serandour, G., Kerschen, G. Golinval, J.-C., "Nonlinear normal modes, Part II:Toward a practical computation using numerical continuation techniques", *Mechanical Systems and Signal Processing*, 23, 195-216, 2009.

[28] Pyragas, K., "Continuous control of chaos by self-controlling feedback", *Physics Letters A*, 170, 421-428, 1992.

[29] Sciavicco, L., Modeling and control of robot manipulators, *Springer*, London, 2000.

[30] Seydel, R., Practical bifurcation and stability analysis, *Springer*, 2010.

[31] Shinbrot, T., "Chaos: Unpredictable yet controllable?", *Nonlinear Science Today*, 3, 1-8, 1993.

[32] Siciliano, B. and Sciavicco, L., Robotics: Modelling, Planning and Control, *Springer*, 2009.

[33] Sinha, S. C. and Joseph, P., "Control of general dynamic systems with periodically varying parameters via LyapunovFloquet transformation", *ASME Journal of Dynamcal Systems, Measurement, and Control*, 116, 650-658, 1994.

[34] Steeb, W. H., The nonlinear workbook, *Word Scientific*, 2008.

[35] Szumiński, P. and Kapitaniak, T. "Stability regions of periodic trajectories of the manipulator motion," *Chaos, Solitons and Fractals*, **17**: 67-78, 2003.

[36] Szumiński, P. and Kapitaniak, T., "Vibrations induced during a stability loss of periodic trajectories of the manipulator", *Machine Dynamics Problems*, 28(2), 65-85, 2004.

[37] Szumiński, P., "Determination of the stiffness of rolling kinematic pairs of manipulators", *Mechanisms and Machine Theory*, 42(9), 1082-1102, 2007.

[38] Tokhi, M.O and Azad, A.K.M., "Modelling of a single-link flexible manipulator system: theoretical and practical investigations", *Robotica*, 14, 91-102, 1996.

[39] Wang, H. O. and Abed, E. H., "Bifurcation control of a chaotic system", *Technical Report*, Institute of Systems Research, University of Maryland, Maryland, 1994.

[40] Wang, Z. and Chau, K. T. (2008). Anti-control of chaos of a permanent magnetic DC motor system for vibratory compactors. *Chaos, Solitons and Fractals*, **36**: 694-708.

[41] Wang, R. and Jing, Z., "Chaos control of chaotic pendulum system", *Chaos, Solitons and Fractals*, 21, 201-207, 2004.

[42] Wing-Kuen Ling, B., Ho-Ching Lu, H., Lam, H., "Control of chaos in nonlinear circuits and systems", *World Scientific Series on Nonlinear Science, Series A*, 64, 2009.

[43] Yu, P., "Closed-form conditions of bifurcation points for general differential equations", *International Journal of Bifurcation and Chaos*, 15, 1467-1483, 2005.